Constraints on the timing of debris-covered and rock glaciers: an exploratory case study in the Hólar area, northern Iceland

José M. Fernández-Fernández[(1)], David Palacios[(1)], Nuria Andrés[(1)], Irene Schimmelpfennig[(2)], Luis M. Tanarro[(1)], Skafti Brynjólfsson[(3)], Francisco J. López-Acevedo[(1)], Þorsteinn Sæmundsson[(4)], ASTER Team[(2)]

[(1)] High Mountain Physical Geography Research Group. Department of Geography, Complutense University of Madrid, 28040 Madrid, Spain.

[(2)] Aix-Marseille Université, CNRS, IRD, INRA Coll. France, CEREGE, Technopôle de l'Environnement Arbois-Méditerranée, BP 80, 13545 Aix-en-Provence, France.

[(3)] Icelandic Institute of Natural History, Borgum vid Norðurslóð, Box 180, 602 Akureyri, Iceland.

[(4)] Faculty of Life and Environmental Science, University of Iceland, Askja, Sturlugata 7, 101 Reykjavík, Iceland.

Keywords: Iceland; deglaciation; rock glaciers; debris-covered glaciers; ^{36}Cl surface exposure dating.

1. Introduction

Rock glaciers and debris-covered glaciers are indicative of important tipping point phases in regional climatic and geomorphological evolution (Winkler and Lambiel, 2018; Anderson et al., 2018a). An appropriate differentiation between them allows the understanding of their origin, the palaeoclimatic implications and the geomorphological processes that led to their formation. In this work we follow the differentiation between debris-covered glaciers and rock glacier features proposed by Janke et al. (2015), which can also be applied to their derived landforms, once the internal ice has disappeared in

both cases (Fernández-Fernández et al., 2017a). According to this differentiation, the debris-covered glacier surface is characterized by a rock mantle with variable thickness but overall increasing towards the toe (Janke et al., 2015). Commonly, it shows the presence of longitudinal ridges, no features derived from viscous flow (Clark et al., 1994) and depressions derived from thermokarst and collapse (Janke et al., 2015). The existence of central and lateral moraines is also common (Clark et al., 1994). On the other hand, rock glaciers commonly include transversal ridges and furrows derived from compressive flow and the overlap of shear planes among other processes concerning to the debris supply (Janke et al., 2015). Rock glaciers often show some longitudinal ridges resulting from the inclusion of lateral moraines of the original glacier, and also a steep front whose junction with the gentle rock glacier surface is very sharp (Janke et al., 2015).

The existence and dynamics of rock glaciers may indicate permafrost in the region and a Mean Annual Air Temperature (MAAT) ≤ -4 °C at present or in the past if they are relict rock glaciers (e.g. Barsch, 1996). Also, they act as fingerprints of the climatic development (i.e., climate warming or moisture supply decrease, and the subsequent mass balance trend) that led to the transformation from debris-free glaciers to rock glaciers (Johnson, 1980; Giardino and Vitek, 1988; Ackert Jr., 1998; Janke et al., 2015; Anderson et al., 2018a; Kenner, 2018 and others), except rock glaciers which have no relationship with a glacial origin (e.g. Barsch, 1996). In this sense, they are affected by the climatic development during their active period (Humlum, 1998; Berger et al., 2004, Paasche et al., 2007; and others), e.g. when an increase in MAAT can either accelerate (Delaloye et al., 2008; Kellerer-Pirklbauer, 2012; Kellerer-Pirklbauer and Kaufmann, 2012; Kellerer-Pirklbauer et al., 2017; Wirz et al., 2016; Eriksen et al., 2018; Kenner,

2018) or stagnate the rock glacier motion (Emmer et al., 2015; Tanarro et al., 2019). Moreover, rock glaciers also reflect the geomorphological changes of the slopes surrounding the rock glaciers (Humlum, 2000a, Humlum, 2000b), which can transform these rock glaciers without any direct relationship with climatic changes (Deline et al., 2015; Anderson and Anderson, 2016). And finally, these formations are also indicative of the amount of water supplied to the rock glaciers (Kenner et al., 2018; Jones et al., 2018).

Existence and development of debris-covered glaciers can also indicate climatic and geomorphological changes, such as their origin in the transformation from a debris-free glacier caused by an increase in ablation, the intensification of the geomorphological processes in the surrounding slopes, or the combination of both factors (Kirkbride, 2000, Kirkbride, 2011; Brenning, 2005; Azócar and Brenning, 2010; Mayr and Hagg, 2019). Climate changes can also trigger changes in the dynamics of debris-covered glaciers (Hambrey et al., 2008; Benn et al., 2012; Pelto et al., 2013; Glasser et al., 2016). Nevertheless, these changes may also be due to variations in the debris supply derived from the geomorphological activity on the slopes (Anderson and Anderson, 2016; Anderson et al., 2018a; Mayr and Hagg, 2019). In fact, this dual dependence greatly complicates the interpretation of the changes that debris-covered glaciers undergo (Gibson et al., 2017). In this sense, debris-covered glaciers can evolve to rock glaciers throughout various phases driven by climatic evolution and increased debris supply in their environment (Janke et al., 2015; Monnier and Kinnard, 2015; Andrés et al., 2016; Anderson et al., 2018a; Mayr and Hagg, 2019).

77 Climatic changes, as well as changes in the geomorphological dynamics of the slopes,
78 can directly influence the dynamics of the debris covered glacier and rock glaciers
79 (Anderson et al., 2018a), even leading to the stop of their flow stop or complete melt of
80 their internal ice and stabilization of their deposits (Potter et al., 1998; Janke et al.,
81 2013; Emmer et al., 2015; Tanarro et al., 2019). However, it is very difficult to
82 determine when this transformation occurred (Barsch, 1996; Haeberli et al., 2006). In
83 the light of the presently ongoing global warming, it is particularly important to know
84 the trend and evolution of these formations and their relation with climate change, as
85 they have been highlighted as authentic water reservoirs (Rangecroft et al., 2015).

86

87 Recent intensified studies focus on monitoring dynamics (e.g. mobility) of rock glaciers
88 and debris-covered glaciers on a very reduced time scale, but with increasingly
89 sophisticated techniques (Benn et al., 2012; Bosson and Lambiel, 2016; Capt et al.,
90 2016; Emmer et al., 2015; Lippl et al., 2018; Kenner et al., 2018). In spite of the great
91 potential of long-timescale understanding that the dating of active, static or relict rock
92 glaciers and debris-covered glaciers might allow, it has attracted little attention of
93 researchers in recent years in contrast with debris-free glacial chronology, for example,
94 throughout all of North America, where rock glacier landforms are common (Phillips,
95 2016; Briner et al., 2017; Leonard et al., 2017; Vázquez-Selem and Lachniet, 2017;
96 Licciardi and Pierce, Licciardi and Pierce, 2018).

97

98 The timing of formation of rock glaciers and debris-covered glaciers is often deduced
99 by extrapolating their current dynamics to the past (Ackert Jr., 1998; and many other
100 subsequent studies), without considering the dynamic and morphological changes that

these formations can undergo over time (Tanarro et al., 2019). Regional studies have traditionally framed the relative age of rock glaciers within the context of glacial evolution, with support from lake and moraine soil radiocarbon dating (Benedict, 1973; Ribolini et al., 2007 and others).

The need to apply more reliable dating methods to rock glaciers has been proposed for years (Haeberli et al., 2003). Dating rock glaciers methods include:

(i) Lichenometry, from the measurements of lichen growth, the method most commonly applied to rock glaciers (Benedict, 1973; Konrad and Clark, 1998; Galanin et al., 2014 and others) obtains the stabilization point in time of the boulders, within an age range of the last few hundred years, although its application to rock glaciers presents many difficulties (Rosenwinkel et al., 2015). In any case, it only provides reliable results when independent fixed control points (e.g. historical evidence) are available.

(ii) Radiocarbon dating of lacustrine sediment overridden by rock glaciers (Paasche et al., 2007) or dendrochronology of tree trunks buried by rock glacier debris (Bachrach et al., 2004), although these circumstances very seldomly exist.

(iii) Schmidt Hammer dating to determine the stabilization age of rock glaciers from the rock weathering. As in the case of lichenometry, require complex complementary information to determine the minimum stabilization age, and especially independent

123 fixed points (e.g. surface exposure ages; Matthews et al., 2013; Scapozza et al., 2014;
124 Winkler and Lambiel, 2018).

125

126 (iv) Luminescence dating, a method which also presents serious complications of
127 interpretation when applied to rock glaciers (Fuchs et al., 2013).

128

129 Over the last ten years, Cosmic-Ray Exposure (CRE) dating methods using beryllium-
130 10 (10Be), helium-3 (3He) and chlorine-36 (^{36}Cl) have been applied to rock glaciers and
131 debris-covered glaciers, although this approach is far from being routine. 10Be dating
132 has been applied successfully to date stabilization time of rock glaciers in Scotland
133 (Ballantyne et al., 2009), the Alps (Hippolyte et al., 2009) and the Iberian Peninsula
134 (Palacios et al., 2017; Rodríguez-Rodríguez et al., 2017; Andrés et al., 2018a).
135 Correlation between 10Be ages and Schmidt Hammer rebound (R- values) to date rock
136 glaciers was shown by Winkler and Lambiel (2018). 10Be dating has also been applied
137 to date the stabilization of fossil debris-covered glaciers (Fernández-Fernández et al.,
138 2017a) and rock avalanche events on active debris-covered glaciers (Deline et al.,
139 2015). 3He has been applied to study the dynamics of debris-covered glaciers (Mackay
140 and Marchant, 2016). ^{36}Cl dating has been successfully applied to date the stabilization
141 period of several rock glaciers in the Iberian Peninsula (Palacios et al., 2012, Palacios et
142 al., 2015a, Palacios et al., 2015b, Palacios et al., 2016), the Alps (Moran et al., 2016);
143 and the Karçal Mountains in the Lesser Caucasus (Dede et al., 2017).

144

145 However, a recent application of the CRE methods has shown that boulders on the
146 surface of rock glaciers and debris-covered glaciers with limited flow may have

147 received cosmic radiation before their definitive motionless (Mackay and Marchant,
148 2016). In fact, active rock glacier ice can be very old; e.g. radiocarbon dating of plant
149 macrofossil remains in a rock glacier core in the Alps yielded an age of >10 ka (Krainer
150 et al., 2015). 10Be dating of boulders from cold based debris-covered glaciers in
151 Antarctica allowed to deduce that the ice is >1 Ma (Mackay and Marchant, 2016) or
152 even >2 Ma old (Bibby et al., 2016). However, it has also been shown that due to the
153 limited trajectory and erosion of the boulders in a rock glacier, they may retain nuclide
154 inheritance prior to deposition (Çiner et al., 2017).

155

156 ^{36}Cl dating has been successfully applied to basalts, which is the predominant bedrock
157 in Iceland (Swanson and Caffee, 2001; Phillips, 2003; Principato et al., 2006; Licciardi
158 et al., 2006, Licciardi et al., 2007, Licciardi et al., 2008; Schimmelpfennig, 2009;
159 Schimmelpfennig et al., 2009, Schimmelpfennig et al., 2011) has been employed in
160 northern Iceland to date the deglaciation (Principato et al., 2006; Brynjólfsson et al.,
161 2015; Andrés et al., 2018b).

162

163 The Tröllaskagi peninsula, in central north Iceland, hosts a total of 167 rock glaciers,
164 debris-covered glaciers and a few debris-free, mostly north-facing (Sigurðsson and
165 Williams, 2008; Icelandic Meteorological Office, 2018; Fig. 1). They are occupying
166 cirques under similar climatic and geomorphological conditions (Björnsson, 1991;
167 Björnsson and Pálsson, 2008). Two of the cirques in the Víðinesdalur valley
168 (Tröllaskagi peninsula) are occupied by rock glaciers and debris-covered glaciers
169 respectively, namely the Fremri-Grjótárdalur cirque, hosting a large rock glacier
170 complex, and the Hóladalur cirque, hosting a large debris-covered glacier,

Hóladalsjökull. A similar debris-covered glacier exists in the Hofsdalur cirque. These rock glaciers and debris-covered glacier have attracted the attention of researchers to determine their flow dynamics (Wangensteen et al., 2006; Farbrot et al., 2007; Kellerer-Pirklbauer et al., 2007; Lilleøren et al., 2013; Tanarro et al., 2019; Campos et al., 2019), but CRE dating methods have not yet been applied (Fig. 1). A combination of multi-temporal aerial photo imagery, lichenometric procedures and ^{36}Cl dating has recently been applied to study the evolution of two nearby debris-free glaciers during late Holocene (Fernández-Fernández et al., 2019).

Here we will present the results of CRE dating of fossil and active rock glacier and debris-covered glacier deposits, which was preceded by high-accuracy boulder tracking measurements of active rock glaciers and debris-covered glaciers, with the objective to relate the results to the stability degree of the analyzed features. The aim of this work is to (i) test the application of CRE dating to determine the stabilization of rock glaciers and debris-covered glaciers of the Tröllaskagi peninsula; and (ii) investigate their evolution to evaluate the potential for future research contributing to our knowledge of the climatic and glacial evolution in this region.

2. Geographic setting.

The Fremri-Grjótárdalur and Hóladalur cirques in the Víðinesdalur valley, and the Hofsdalur and Héðinsdalur valleys are the focus area of this study and are located in the surroundings of the village of Hólar, on the western side of the Tröllaskagi peninsula. These valleys are tributaries to the main valley of Hjaltadalur, which drains into Skagafjörður (Fig. 1), and host both debris-free, debris-covered and rock glaciers. The summits surrounding these cirques form a flat plateau at around 1200–1330 m a.s.l., hosting flat-bottomed cirques with steep 100–170 m high slopes. These cirque walls are composed of Tertiary basalt bedrock, with semi-horizontal lava flows often separated by

196 30–50 cm thick argillaceous sedimentary layers (Sæmundsson et al., 1980). These walls
197 might have been unstable, as in the rest of Tröllaskagi, and thus are affected by rock slope
198 failures (Jónsson, 1976; Whalley et al., 1983; Mercier et al., 2013; Cossart et al., 2014;
199 Feuillet et al., 2014; Decaulne et al., 2016; Sæmundsson et al., 2018).

200

201 The snouts of the debris-covered and rock glaciers in Tröllaskagi are found at 900–
202 950 m a.s.l., where the MAAT is −1.8 to −2.6 °C (Kellerer-Pirklbauer et al., 2007) and
203 precipitation around 1500–2000 mm (Crochet et al., 2007). The continuous permafrost
204 limit is located between 850 and 950 m a.s.l. (Wangensteen et al., 2006; Etzelmüller et
205 al., 2007; Czekirda et al., 2019). The current ELA of the main debris-free glaciers close
206 to the study cirques is 1010–1060 m a.s.l., with the MAAT around −2.3 °C (Fernández-
207 Fernández et al., 2017b). These glaciers reached their LIA maximum ca. 1865–1900,
208 according to Caseldine (1985) or in the 15th century or earlier according to Fernández-
209 Fernández et al. (2019). During this maximum the ELA was about 950–1010 m a.s.l. and
210 the MAAT 1.7–1.9 °C lower than at present (Caseldine and Stötter, 1993; Fernández-
211 Fernández et al., 2017b).

212 **3. Previous research on the study area.**

213 CRE dating (Andrés et al., 2018b), combined with previous radiocarbon results (see
214 synthesis in Pétursson et al., 2015), indicates that the glacier outlet of the Skagafjörður
215 fjord (Fig. 1), flowing down from the Icelandic Ice Sheet (IIS), was situated in the
216 outermost sector of the fjord at approximately 17–15 ka. Subsequently, this glacier
217 outlet retreated and occupied the central part between 15 and 12 ka, and then the
218 innermost part of the fjord around 11 ka. After 11 ka, rapid deglaciation affected the
219 fjord, when the IIS outlet glacier almost reached dimensions similar to the current

Hofsjökull ice-cap in central Iceland. Norðdahl, 1991a, Norðdahl, 1991b emphasized that most of the Tröllaskagi valleys run N-S, thus facilitating the flow of the IIS outlets, but important secondary valleys in these mountains were outside these flows. Ingólfsson (1991) and Norðdahl, 1991a, Norðdahl, 1991b summarized the studies carried out on the possible glaciation of the Tröllaskagi summits and show how most geomorphologists and palaeobotanists in the early 20th century argued for an ice-free scenario for these summits during the LGM. This hypothesis was supported by simulation models (Hubbard et al., 2006). In fact, ice-free plateaus on the Tröllaskagi summits during the LGM may have served as refugia for flora and fauna (Rundgren and Ingólfsson, 1999).

The first study area of this paper includes the two main cirques in the Víðinesdalur valley: Fremri-Grjótárdalur and Hóladalur (Fig. 1, Fig. 2). In the Fremri-Grjótárdalur cirque, two lower relict rock glacier sectors have been differentiated, overlapped by active rock glaciers in the western and eastern sectors of the cirque (Andrés et al., 2016; Farbrot et al., 2007; Kellerer-Pirklbauer et al., 2007). The whole rock glacier complex occupies an area of 0.96 km2 with a maximum length of 1 km and a maximum width of almost 300 m. These rock glaciers show typical features, i.e. transverse ridges and furrows composed of large angular boulders (Kellerer-Pirklbauer et al., 2007). The collapsed fronts of the relict rock glaciers descend to an altitude of 850 m a.s.l., while the steep fronts of the active ones descend to 950 m a.s.l. (Tanarro et al., 2018, Tanarro et al., 2019). The existence of interstitial ice in the active rock glaciers and the non-existence of ice in the relict rock glaciers have been demonstrated by geophysical surveys and field observations in previous works (Farbrot et al., 2007; Kellerer-Pirklbauer et al., 2007; Tanarro et al., 2018, Tanarro et al., 2019).

The Hóladalsjökull glacier, located in the adjacent cirque to the east of Fremri-Grjótárdalur (Fig. 1), is formed by a debris-covered lower section, 2 km long and 1.3 km-wide, covering an area of 2.2 km2. The front is located at 900 m a.s.l. The upper sector is formed by 1.7 km-long debris-free glacial ice, occupying an area of 2.5 km2 (Tanarro et al., 2018, Tanarro et al., 2019). Previous works described the existence of glacial ice, up to 20 m thick, under a meter-thick debris in the debris-covered sector of Hóladalsjökull glacier, which was visible at its forehead and in collapsed depressions (Andrés et al., 2016; Tanarro et al., 2018, Tanarro et al., 2019).

The age and origin of these rock glaciers and debris-covered glaciers is still under discussion. The ages of their inner and outer lobes age have been assumed to be between 5 and 9 ka for headwall recession rates estimation (Farbrot et al., 2007). Through streamline interpolations from present surface velocities, Wangensteen et al. (2006) estimated the maximum age of the rock glaciers to be about 4.5–5 ka BP, with reactivation of the higher lobes about 1.0–1.5 ka BP. Using a combination of the same method and Schmidt hammer dating, Kellerer-Pirklbauer et al., 2007, Kellerer-Pirklbauer et al., 2008 proposed an age contemporary with the 8.2 ka event (8.6–8.0 ka cal. yr BP according to Greenland stratigraphy; Alley and Ágústsdóttir, 2005) for Fremri-Grjótárdalur relict rock glaciers. Kellerer-Pirklbauer et al. (2007) proposed that the origin of the active rock glacier was related to one of the first neoglacial advances in Tröllaskagi at about 5.9–5.2 cal ka. BP, with reactivation during a second neoglacial advance by 3.2–3.0 ka (Kellerer-Pirklbauer et al., 2007). From a combination of headwall recession rate and lichenometric dating, the Nautárdalur rock glacier, located a few kilometers to the east, was considered to be about 0.2 ka old and related to the Little

Ice Age glacial expansion (Martin et al., 1994; Hamilton and Whalley, 1995a, Hamilton and Whalley, 1995b).

The dynamics of these rock and debris-covered glaciers are under discussion. Using data obtained by digital photogrammetry, Wangensteen et al. (2006), proposed horizontal block displacement rates ranging from <0.10 to a maximum of 0.84 m yr^{-1} in the Hóladalsjökull debris-covered glacier and a maximum of 0.74 m yr^{-1} in the Fremri-Grjótárdalur rock glacier. Kellerer-Pirklbauer et al. (2007) used similar techniques in the Fremri-Grjótárdalur rock glacier and obtained rates of 0.06–0.74 m yr^{-1}. Lilleøren et al. (2013), used satellite radar interferometry and reported block displacement rates of 0.2–0.5 m yr^{-1} in some rock glaciers in Tröllaskagi. Tanarro et al. (2019) applied jointly manual and digital photogrammetry, obtaining a mean horizontal displacement rate of 0.33 m yr^{-1} for the Hóladalsjökull debris-covered glacier, mainly connected to surface lowering processes derived from ice degradation, and insignificant movement for the Fremri-Grjótárdalur rock glacier. These results are similar to those obtained in the Nautárdalur glacier, where boulder movement measured by theodolite during a 17-year period ranged from <0.05 m to 0.31 m yr^{-1}, with the snout advancing <1 m during this period (Whalley et al., 1995a, Whalley et al., 1995b).

The second study area, Hofsjökull glacier, is located at the head of the Hofsdalur valley, to the south of Hólardalur (Fig. 1). Hofsjökull glacier is a 1.7 km long and 1.5 km wide debris-covered lower section and 1.3 km long debris-free upper section. Hofsjökull glacier has a thickness ratio of glacial ice and debris similar to Hóladalsjökull glacier (Campos et al., 2019). Campos et al. (2019) found average horizontal boulder

293 displacement rates of 0.22 m yr^{-1} in Hofsjökull glacier, and 0.15 m yr^{-1} in the nearby
294 Júllogil rock glacier, which confirms the stability of these glaciers whose predominant
295 dynamic is the subsidence associated to ice downwasting.

296

297 The third study area is Héðinsdalsjökull in Héðinsdalur valley (Fig. 1), to the south of
298 Hofsdalur. The distal sector of Héðinsdalsjökull is a debris mantle that evidences former
299 extent of a debris-covered glacier. The snout of this palaeo debris-covered glacier is at
300 640 m a.s.l. The present debris-covered glacier extends from 900 m a.s.l. upwards,
301 where ice-collapsed depressions can be observed on a debris mantle. The total debris-
302 covered sector (with and without underlying ice) is 2.1 km long, with the collapsed and
303 active sectors being 1.2 and 0.9 km long, respectively. The upper sector is formed by
304 debris-free glacial ice 2.3 km long and 2.6 km wide.

305 **4. Methods**

306 *4.1 Geomorphological setting and CRE sampling strategy*

307 The three complementary methodological steps of this research focused on the Fremri-
308 Grjótárdalur rock glaciers and the Hóladalsjökull, Hofsjökull and Héðinsdalsjökull
309 debris-covered glaciers. The first step was to determine when the deglaciation occurred
310 in these valleys and in each of the two cirques. The second step was to determine the
311 exposure age of the boulders of the relict rock glaciers located in the Fremri-
312 Grjótárdalur cirque. In this context, the relict rock/fossil debris-covered glaciers are
313 representative of the first landforms originated after deglaciation inside the cirques. The
314 application of this strategy, following a clear chronological sequence indicated by the
315 geomorphological landform disposition, will allow the reconstruction of the
316 deglaciation phases and the rock glacier formation.

The final step was to determine the stabilization period of the frontal boulders of the debris-covered glaciers that still conserve underlying ice, and those without it. For sufficiently representative sampling, we took samples from boulders of both the Hofsjökull and Héðinsdalsjökull debris-covered glaciers. By this way, we will be able to deduce whether the stabilization moment of these debris-covered glaciers was synchronous in different valleys of Tröllaskagi.

Previous to CRE sampling of the fronts at the active debris-covered glaciers and rock glaciers, a photogrammetric analysis was applied to these boulders to measure their horizontal displacement and hence their stability degree in the last decades, in order to avoid that high-mobility or potentially overturned boulders are sampled.

Samples were taken from gentle flat-topped surfaces by using hammer and chisel, preferring boulders with a > 1-m diameter and with signs of glacial polishing which minimize the risk of cosmogenic nuclide inheritance.

4.2 Movement analysis of the sampled boulders

To determine the degree of stability of the boulders sampled for CRE dating, we followed the method previously proposed by Tanarro et al. (2019). We applied digital photogrammetry to historical aerial photographs to determine the horizontal movement and elevation changes of sampled boulders from debris-covered glaciers and rock glaciers. This method was applied to the rock glacier in Fremri-Grjótárdalur, and the debris-covered glacier, the Hofsjökull, to complement previous analyses of boulder movement in the area (Tanarro et al., 2019; Campos et al., 2019). We used photo stereo pairs from 1980 and 1994, which were the only flights available with sufficient

resolution quality to identify the same boulders in both years. The photo stereo pairs were scanned at a high resolution (20 and 15 μm respectively). A digital photogrammetric workstation was used to correct the geometric deformation of the photograms and to create stereoscopic models for both dates. In this process, the absolute orientation was obtained from a series of control points from an orthophoto of the year 2000. To estimate the uncertainty (RMSExyz) on the boulder tracking in rock glaciers and debris-covered glaciers, X, Y and Z values of moraine boulders that are considered stable and immobile were determined. The resulting RMSExyz values are at most 0.32 m. The photograms covering the area of the Fremri-Grjótárdalur and Hóladalsjökull cirques present a slightly lower error range (RMSExyz 0.15–0.25 m) than those covering the Hofsdalur cirque (RMSExyz 0.17–0.32 m). With the stereoscopic models from both dates, we carried out 3D photogrammetric restitution of a set of boulders identified on the surface of the sampled landforms (see the boulders tracked and the geomorphological units to which they belong in Table 1). Some of these boulders were the same boulders as those sampled for CRE dating and others were very close to them in the same geomorphological unit (Fig. 2, Fig. 3, Fig. 4). Finally, we compiled a database including X and Y coordinates, and altitude (Z) of each boulder in both dates. These data were then processed to obtain the horizontal displacement and elevation difference for each boulder.

4.3 ^{36}Cl CREdating

The locations of the 18 CRE samples are shown in Table 2 and Fig. 3, Fig. 4, Fig. 5. Samples HOL-1, HOL-2, FGD-1, FGD-2 and FGD-11 were collected during a fieldwork conducted in 2012. Preliminary results of these first samples were presented in Andrés et al. (2016), but the age re-calculation with the new calculator (Schimmelpfennig et al., 2009) and different in situ ^{36}Cl production rates (detailed below) considerably improved

366 the results. These samples were crushed and sieved in the "Physical Geography
367 Laboratory" of the Complutense University of Madrid (Spain), and the 0.25–1 mm
368 fraction was separated. Aliquots splits of rocks were taken for chemical analysis both
369 from the pre-treated samples (bulk fraction; Table 3) and the samples after a first pre-
370 dissolution conducing to the removal of Cl-rich ground mass (Table 4). Chemical analysis
371 were carried out at the "Activation Laboratories" (Ancaster, Canada). Chemical
372 processing of the samples was carried out at the "PRIME Laboratory" (Purdue University,
373 USA), following the procedures described in Zreda et al. (1999) and Phillips (2003) for
374 the ^{36}Cl extraction from whole rock. The resulting targets were analyzed using accelerator
375 mass spectrometry (AMS) to determine the $^{35}Cl/37Cl$, $^{36}Cl/^{35}Cl$ and $^{36}Cl/37Cl$ ratios. Two
376 chemistry blanks (Cblk3125-1 and Cblk3125-2) were processed together with the
377 samples, for which the laboratory provided only the data collected in Table 5, with the
378 previously calculated results of Cl and ^{36}Cl concentrations, which were used here to
379 calculate the ^{36}Cl ages.

380 A second batch of samples, ELLID-1, ELLID-2, FGDsingle bond1B, FGDsingle bond2B,
381 FGDsingle bond3B, FGDsingle bond4B, FGDsingle bond5B, HOFS-1, HOFS-2, HOFS-
382 3, HEDIN-1, HEDIN-2 and HEDIN-3 were sampled in 2014 and 2015. The initial
383 mechanical preparation was also carried out in the "Physical Geography Laboratory"
384 (Complutense University of Madrid, Spain) and the 0.25–1 mm fraction was chemically
385 processed in the Laboratoire National des Nucléides Cosmogéniques (LN2C) at the
386 "Centre Europeén de Recherche et d'Enseignement des Géosciences de l'Environnement"
387 (CEREGE), in Aix-en-Provence (France). Aliquot splits of bulk rock were taken from
388 several representative samples of each study area, in order to analyze the concentrations
389 of major and trace elements (Table 3) at the "Service d'Analyse des Roches et des
390 Mineraux" (SARM, Nancy, France). After removing dust and fines and etching the

391 samples with nitric (HNO3) and hydrofluoric (HF) acids, aliquots were taken again to
392 measure the target element concentrations by inductively coupled plasma-optical
393 emission spectrometer (ICP-OES) at SARM (Table 4). An ^{35}Cl-enriched spike (~99%)
394 was then added to the samples for isotope dilution (Ivy-Ochs et al., 2004) and the samples
395 were completely dissolved in a mixture of HF + HNO3. The undissolved fines and
396 fluoride gel was removed after centrifugation of the samples. The following steps of the
397 process follow the procedure proposed by Schimmelpfennig et al. (2011). Finally,
398 measurements of the ^{35}Cl/37Cl and ^{36}Cl/^{35}Cl ratios were carried out at the "Accélérateur
399 pour les Sciences de la Terre, Environnement et Risques" (ASTER, CEREGE), to infer
400 the concentrations of ^{36}Cl and Cl. Three chemistry blanks (BK-1, BK-2 and BK-3) (Table
401 5) were processed together with the samples.

402

403 The Excel™ spreadsheet proposed by Schimmelpfennig et al. (2009) was used to
404 calculate ^{36}Cl exposure ages. The most relevant data used in the calculations (topographic
405 shielding factor, sample thickness, chemical composition of the samples) are summarized
406 in Table 2, Table 3, Table 4. In absence of lab density measurements, a value of
407 2.7 g cm−3 is assumed for all samples. The nucleonic and muonic scaling factors based
408 on the time-invariant "St" scheme (Stone, 2000) were applied, and the topographic
409 shielding factor was calculated with the ArcGIS toolbox designed by Li (2018), since the
410 data could not be taken directly in the field due to fog. The exposure age calculations
411 were made with the following ^{36}Cl production rates: 57.3 ± 5.2 atoms ^{36}Cl (g Ca)$^{-1}$ yr^{-1}
412 for spallation of Ca (Licciardi et al., 2008), 148.1 ± 7.8 atoms ^{36}Cl (g K)$^{-1}$ yr^{-1} for
413 spallation of K (Schimmelpfennig et al., 2014), 13 ± 3 atoms ^{36}Cl (g Ti)$^{-1}$ yr^{-1} for
414 spallation of Ti (Fink et al., 2000), 1.9 ± 0.2 atoms ^{36}Cl (g Fe)$^{-1}$ yr^{-1} for spallation of Fe
415 (Stone et al., 2005), and 696 ± 185 neutrons (g air)$^{-1}$ yr^{-1} for the production rate of

416 epithermal neutrons from fast neutrons in the atmosphere at the land/atm interface
417 (Marrero et al., 2016). A high-energy neutron attenuation length of 160 g cm−2 was
418 applied.

419

420 **5. Results**

421 *5.1 Movement of boulders from rock glaciers and debris-covered glaciers.*

422 The results of the horizontal movement and elevation changes of the analyzed boulders
423 are presented in Table 1. Their locations are shown in Fig. 2, Fig. 3, Fig. 4.

424

425 The moraine boulders HOL-1 and HOL-2, located in the Hóladalsjökull cirque, have
426 remained stable during the 14-year observation period. Horizontal movement (0.052 and
427 0.022 m yr^{-1}) and elevation changes (−0.04 and 0.06 m yr^{-1}) are negligible and within the
428 RMSE of our analysis. We obtained similar results from the analysis of the moraine
429 boulders in the Fremri-Grjótárdalur cirque, where sample FDG-11 was collected. There
430 is the exception of one boulder, which indicates a slight horizontal movement of
431 0.108 m yr^{-1}, while the rest hardly show any movement, with maximum about
432 0.05 m yr^{-1}.

433

434 We obtained similar results from the boulders located on the ridges at the Fremri-
435 Grjótárdalur relict rock glaciers. For example, in the western rock glacier from which
436 samples FDG-1 and FDG-2 were collected, we obtained displacement rates of
437 <0.047 m yr^{-1} and maximum elevation difference of −0.43 m yr^{-1}. In the eastern rock
438 glacier, we obtained a movement of 0.022 m yr^{-1} for the samples FGD-4B and FGDsingle

bond5B, and maximum elevation changes of −0.36 m yr^{-1}. In any case the total horizontal displacement during the 1980–1994 was not higher than 0.66 m (Table 1).

As it would be expected, different results were obtained from the boulders located on the ridges of the active rock glaciers (representative for samples FGDsingle bond1B, FGD-2B and FGDsingle bond3B), although the movement is very slow, between 0.076 m yr^{-1} and maximum 0.16 m yr^{-1}. These values, therefore, would indicate displacements of 1.06 and 2.2 m in 14 years. The elevation differences are negative, but negligible, between −0.04 and − 0.19 m yr^{-1}.

We also obtained very small displacements on the front of the Hofsjökull debris-covered glacier (boulders from which samples HOFS-1, HOFS-2 and HOFS-3 were collected). The horizontal displacement rates of the boulders range from 0.18 m to 0.37 m yr^{-1}, indicating about 2.5 and 5.16 m displacement and elevation changes of −0.19 to −1.26 m in 14 years.

5.2 Deglaciation of the Tröllaskagi internal valleys: geomorphology and CRE dating results

Fieldwork and moraine mapping were carried out in the Víðinesdalur, Hofsdalur and Héðinsdalur valleys, during the summers of 2012, 2014 and 2015, exploring for erratic boulders or glacially polished bedrock surfaces suitable for applying CRE dating. The abundance of debris-flows and other slope processes have transformed and covered the glacial landforms of the valley. No bedrock outcrops, or any existing outstanding block in the relief were observed, with the exception of those generated by post-glacial rock

avalanches. The only exceptions observed during the fieldwork were two polished bedrocks located on the Elliði ridge (Fig. 5), which separates the Víðinesdalur valley to the south from the Kolbeinsdalur valley to the north (Fig. 6). The polished surfaces are at around 600 m a.s.l., i.e. 300 m above the bottom of the Víðinesdalur valley. Samples were collected from each of these polished surfaces (ELLID-1 and ELLID-2), whose ages indicate the start of deglaciation of the studied valleys. Both samples gave very similar ages: 16.3 ± 1.2 ka (ELLID-1) and 16.3 ± 0.9 ka (ELLID-2), published in Fernández-Fernández et al. (2019).

5.3 Deglaciation of the Tröllaskagi cirques: geomorphology and CRE dating results.

To determine the timing of the deglaciation of the Fremri-Grjótárdalur and Hóladalsjökull cirques, glacial landforms located in front of the rock glaciers and the debris-covered glacier were studied. No polished surfaces are preserved, only remnants of a highly degraded moraine ridge in each cirque. In the Fremri-Grjótárdalur cirque there is a degraded lateral moraine in front of the rock glaciers (Fig. 2, Fig. 7, Fig. 8). One prominent glacial boulder (FDG-11) was considered suitable for exposure dating and yielded an age of 11.3 ± 0.8 ka. A similar highly degraded moraine is located about 900 m distal and 100 m lower in altitude than the Hóladalsjökull debris-covered glacier (Fig. 9). Two large stable blocks with glacially polished surfaces were considered suitable for exposure dating (Fig. 9). From those, samples HOL-1 and HOL-2 yielded ages of 11.1 ± 1.1 and 10.3 ± 0.7 ka respectively (Fig. 6, Fig. 9) (Figs. 6 and 9). The three ages are indistinguishable from each other within their 1 sigma analytical uncertainties, and are in chronostratigraphical order with the ELLID samples (Fig. 6).

5.4 Stabilization of boulders from the relict rock glaciers (with no internal ice): geomorphology and CREdating results.

Two large boulders (samples FDG-1 and FDG-2) were collected at the frontal margin of the relict rock glacier located below the active rock glaciers of the western sector of Fremri Grjótárdalur cirque about 870 m a.s.l. (Fig. 2, Fig. 7, Fig. 8). The samples yielded exposure ages of 10.5 ± 0.7 and 11.1 ± 0.7 ka respectively. Two more boulders (samples FDG-4B and FDGsingle bond5B) yielded ages of 9.3 ± 0.7 and 9.5 ± 0.7 ka respectively. They are located at the frontal edge of the other relict rock glacier at approximately 1005 m a.s.l., about 150 m higher than FDG-1 and FDG-2, in the eastern sector of the cirque (Fig. 2).

5.5 Stabilization of boulders from active rock glaciers and debris-covered glaciers (with stagnant internal ice): CRE dating results.

Three samples were collected from boulders at the front of the active rock glacier, with internal ice, to the western sector of Fremri-Grjótárdalur (FGDsingle bond1B, FGD-2B and FDGsingle bond3B), at an altitude of approx. 960 m (Fig. 2, Fig. 8). These samples gave ages of 2.5 ± 0.2, 5.2 ± 0.4 and 6.5 ± 0.5 ka respectively, in good chronostratigraphical agreement with previous samples of the cirque (moraine and relict rock glacier). To determine the timing of the stabilization of the debris-covered glaciers, three samples were taken from boulders at the frontal part of the Hofsjökull debris-covered glacier, located at the bottom of Hofsdalur. The front of Hofsjökull presents a glacial ice wall of around 20 m, covered by a 2-m-thick debris mantle. Three samples were collected from boulders at the front of the glacier, located at about 900 m a.s.l. (HOFS-1, HOFS-2 and HOFS-3; Fig. 3, Fig. 10). The results of these samples yielded

ages of 5.4 ± 0.5, 5.6 ± 0.5 and 6.7 ± 0.6 ka, respectively. These ages are similar to the samples FGD-2B and FDG-3B from the active rock glaciers.

Finally, three samples were taken from the debris-covered glacier of Héðinsdalur, in the distal sector of Héðinsdalsjökull, where no internal ice persists at present (HEDIN-1, HEDIN-2 and HEDIN-3), at about 650 m a.s.l. (Fig. 4, Fig. 11), and yielded ages of 3.0 ± 0.3, 2.6 ± 0.3 and 2.2 ± 0.2 ka respectively.

5.6. Chronological sequence summary.

The application of ^{36}Cl dating has revealed that the onset of the deglaciation in the main valleys Viðinesdalur and Kolbeinsdalur started around 16 ka. Subsequently, cirque glaciers of Fremri-Grjótárdalur and Hóladalur culminated in a last glacial advance or stillstand at 11 ka, when the moraine abandonment was definitive. Shortly afterwards, the relict rock glaciers of Fremri-Grjótárdalur stabilized in the cirques at around 11–9 ka, while the active debris-covered glacier of Hofsdalur and the rock glaciers of Fremri-Grjótárdalur stagnated at 7–5 ka. And finally, the definitive stabilization of the relict debris-covered glacier of Héðinsdalsjökull occurred at 3–2 ka.

6. Discussion

6.1 Deglaciation of the Tröllaskagi internal valleys and beginning of the formation of the rock glaciers and debris-covered glaciers into the cirques.

The intense degradation of the Tröllaskagi glacial landscape, due to slope mass movements together with the deposition of soil, fluvial, debris-flow and aeolian sediments, which have partly covered the slopes, greatly limits the possibility of obtaining a sufficient number of reliable CRE samples to map/reconstruct the deglaciation pattern

of the three studied valleys. The only samples obtained from the Elliði ridge summits (ELLID-1, ELLID-2) yielded the same age (16.3 ± 1.0 ka) (Fig. 6). This age may indicate the definitive retreat of the glaciers that descended through the Hóladalur valley. The datings of the moraine remains observed in the Fremri-Grjótárdalur and Hóladalur cirques yielded indistinguishable ages of 11.3 ± 0.7, 11.1 ± 1.0 and 10.3 ± 0.7 ka (Fig. 6), which are around 5 ka younger than those from the Elliði ridge.

The results obtained in this study reflect a similar deglaciation pattern to that observed elsewhere in Iceland. In fact, the onset of the deglaciation in Iceland can be determined around 18.6 cal. ka BP, in concordance with the global sea level rise (Andrews et al., 2000; Ingólfsson and Norðdahl, 2001), which increased sharply during the Bølling interstadial (14.7 to 14.1 ka BP), when the Icelandic Ice Sheet IIS collapsed and retreated from the north (Norðdahl et al., 2008; Norðdahl and Ingólfsson, 2015; Pétursson et al., 2015).

The ages obtained in this study suggest that the retreat of the glaciers in Tröllaskagi coincided with the retraction of the main tongue of the IIS in this area, which flowed down from the highlands throughout the Skagafjörður fjord. This glacier retreated from the mouth of the fjord (161 km north of the present Hofsjökull ice-cap) in 15.9 ± 1.2 ka, based on ^{36}Cl dating (Andrés et al., 2018b). This indicates that from the Bølling interstadial, the glaciers in the internal Tröllaskagi valleys and the Skagafjörður IIS outlet glacier were already disconnected. This may show that from the Allerød interstadial (13.9–12.9 ka) at least some of the Tröllaskagi glaciers behaved as alpine glaciers, already disconnected from the IIS. The Tröllaskagi plateau therefore, may have remained ice-

559 free, as it has been widely proposed (Ingólfsson, 1991; Norðdahl, 1991a, Norðdahl,
560 1991b; Rundgren and Ingólfsson, 1999; Andrés et al., 2016).

561

562 Data from lacustrine and marine sediments, and sea level changes, suggest a cold period
563 and glacial advances at the end of the Bølling interstadial, around 14 cal. ka BP
564 (Ingólfsson et al. 1997; Pétursson et al., 2015; Patton et al., 2017). However, probably
565 due to the intense paraglacial erosive activity, there is no geomorphological evidence of
566 that cold episode in the Víðinesdalur valley or in the Fremri-Grjótárdalur and Hóladalur
567 cirques. Lake sediments from the Torfadalsvatn lake, on the Skagi peninsula (west of the
568 Skagafjörður fjord), show that temperatures rose to current levels during the Allerød
569 interstadial in the Skagafjörður area (Rundgren, 1995, 1999; Rundgren and Ingólfsson,
570 1999). The Tröllaskagi glaciers, might have retreated reaching their their minimum extent
571 in their cirques during the Bølling interstadial.

572

573 After the Allerød interstadial, during the Younger Dryas, major degradation of the
574 biosphere and increased amounts of sea-ice occurred in northern Iceland (Rundgren,
575 1995, 1999; Xiao et al., 2017). The glacial outlets descending from the IIS, reoccupied
576 the main fjords of northern Iceland up to their middle parts according to shoreline and
577 tephra distribution (Pétursson et al., 2015). This deglaciation pattern has been confirmed
578 in Skagafjörður with ^{36}Cl CRE ages of 12.7 ± 0.9 and 11.9 ± 0.9 ka BP for polished
579 surfaces, when the front of the glaciers left the middle part of the fjord, 130 km from the
580 current Hofsjökull ice cap (Andrés et al., 2018b). The last important advance or stagnation
581 of the IIS outlets in northern Iceland was around 11 ka (Preboreal), when their fronts were
582 located at the innermost parts of the fjords (Ingólfsson et al., 1997; Norðdahl and
583 Einarsson, 2001; Norðdahl and Pétursson, 2005; Pétursson et al., 2015). ^{36}Cl CRE ages

584 confirm the position of the outlet terminus close to the present shoreline in the
585 Skagafjörður fjord (90 km from the current Hofsjökull ice-cap) at around 11 ka (Andrés
586 et al., 2018b). This last glacial advance was immediately followed by an abrupt retreat
587 until the disappearance of the IIS within the current limits of the glaciers (Kaldal and
588 Víkingsson, 1990; Andrews et al., 2000; Norðdahl and Einarsson, 2001; Geirsdóttir et al.,
589 2002, Geirsdóttir et al., 2009; Larsen et al., 2012; Pétursson et al., 2015; Harning et al.,
590 2016). This has been also confirmed by CRE ^{36}Cl ages in Skagafjörður (Andrés et al.,
591 2018b).

592

593 Samples FDG-11 (11.3 ± 0.7 ka) from the Fremri-Grjótárdalur moraine, and HOL-1
594 (11.1 ± 1.1 ka) and HOL-2 (10.3 ± 0.7, ka) from the moraine in front of Hóladalsjökull
595 glacier (Fig. 6), may represent a glacial advance or glacial front stagnation in the
596 Hóladalur valley during the Preboreal, around 11 ka, similar to that observed at the bottom
597 of the fjords. After this, the Hóladalur glaciers must have retreated very quickly, as
598 occurred in the nearby ice-caps (Andrés et al., 2018b), probably until the total
599 disappearance of all the Icelandic glaciers at ~9 ka (Larsen et al., 2012; Geirsdóttir et al.,
600 2018). This may also be the case of Drangajökull, in the NW (Harning et al., 2016;
601 Anderson et al., 2018b). However, other studies have also suggested that Drangajökull
602 persisted into the early-mid Holocene (Schomacker et al., 2016).

603

604 The ages of the moraine located in front of the Fremri-Grjótárdalur relict rock glaciers
605 (~11.3 ka) and the frontal sector of these rock glaciers (~10.5–11 ka and ~9.4 ka) date to
606 the Early Holocene (Table 4). Note that we do not report mean ages for the rock glacier
607 front as they might have had different exposure histories. These dates demonstrate the
608 rapid transformation of the small debris-free glaciers that occupied the cirque at the

609 beginning of the Holocene into rock glaciers, whose fronts stabilized shortly afterwards.
610 The surface boulders on the frontal area of these rock glaciers seemed to have stabilized
611 rapidly, resulting in undisturbed exposure to cosmic radiation, otherwise younger and less
612 internally coherent ages would have been expected (Fig. 2). Hereafter, we will use the
613 concept of "stabilization" along the discussion assuming that the duration between
614 boulder emplacement and stabilization is insignificant compared to the age of the
615 landforms. The different stabilization ages of the fronts of the western and eastern relict
616 rock glaciers (~10.5–11 ka and ~9.4 ka) may be related to their different altitudes, located
617 around 870 m a.s.l. and between 940 and 990 m a.s.l., respectively: in a warming tendency
618 context, with permafrost altitude rising, the rock glaciers that first become inactive are
619 the lowest (Fig. 8). The similarity of the boulder ages from the relict rock glaciers and
620 those of the moraines makes us confident that the samples are not affected by cosmogenic
621 nuclide inheritance from earlier exposure periods (Andrés et al., 2018b; Fernández-
622 Fernández et al., 2019), which is shown to be an issue in other areas (e.g. Çiner et al.,
623 2017).

624

625 The formation of rock glaciers relatively quickly after the retreat of the glacial fronts from
626 youngest moraines in the cirques may indicate that they derive from the rapid
627 transformation of debris-free glaciers during the final deglaciation stages. After that, their
628 fronts, already evolved to those typical of the rock glaciers, stabilized shortly afterwards
629 as they lost the internal ice (Humlum, 2000a, Humlum, 2000b; Janke et al., 2015; Monnier
630 and Kinnard, 2015; Andrés et al., 2016; and many others). CRE dating of frontal boulders
631 from relict rock glaciers and glacial polished bedrock on which they are supported has
632 demonstrated in many mountain ranges that rock glaciers usually formed shortly after
633 deglaciation, followed by relatively rapid stabilization of their fronts. This process has

been observed in several areas of the Iberian Peninsula, such as Sierra Nevada (Palacios et al., 2016), Sierra de Guadarrama (Palacios et al., 2012), Sierra de la Demanda (Fernández-Fernández et al., 2017a), the Cantabrian Mountains (Rodríguez-Rodríguez et al., 2017), the Central Pyrenees (Palacios et al., 2017) and the Eastern Pyrenees (Andrés et al., 2018a), and also in the British Isles (Ballantyne et al., 2009), the Alps (Hippolyte et al., 2009; Moran et al., 2016), the Karçal Mountains in Lesser Caucasus (Dede et al., 2017) and in the New Zealand Southern Alps (Winkler and Lambiel, 2018).

The rapid formation of debris-covered glaciers and rock glaciers at the end of deglaciation and the early stabilization of their fronts has a logical explanation in many mountains (Winkler and Lambiel, 2018), but especially in the Tröllaskagi valleys (Fig. 12). Deglaciation supposes the decompression of the upper part of the cirque walls from the glacier ice, accelerating paraglacial processes shortly after its deglaciation, as it has been observed in other studied mountains (Ballantyne, 2002, 2009; Mercier, 2008; Oliva et al., 2016). Intense paraglacial activity just after deglaciation has been proposed in many valleys of Tröllaskagi, and it has even been demonstrated by radiocarbon dating of several landslides (Mercier et al., 2013, Mercier et al., 2017; Cossart et al., 2014; Coquin et al., 2015; Decaulne et al., 2016). The intense supply of material from the slopes derived from paraglacial activity can transform a retreating glacier into a rock glacier or debris-covered glacier (Johnson, 1980; Giardino and Vitek, 1988; Ackert Jr., 1998; Janke et al., 2015; Anderson et al., 2018a; among others). In the same way, the end of paraglacial activity may involve stabilization of the rock glacier (Humlum, 2000a, Humlum, 2000b; Deline et al., 2015; Anderson and Anderson, 2016). Our results show that relatively short time passed since the glaciers advanced and formed glacial moraines and the formation and the subsequent stabilization of rock glaciers. If we consider the uncertainty ranges of the

moraine and relict rock glacier stabilization ages (see Fig. 2), this period might have lasted 2–4 ka as maximum. These results support the idea that rock glaciers form during the transformation of glaciers within paraglacial mountain landscape (Knight et al., 2018). However, to explore whether the interstitial ice of these rock glacier comes from glacial ice, as we propose, or from aggradation ice requires other research methods. In that sense, the combination of the field geomorphological survey and chronological analysis with a fabric study (e.g. Ribolini et al., 2007) can shed more light on the formation of the rock glaciers.

6.2 The exposure age of boulders in active rock glaciers and debris-covered glaciers and the climatic and geomorphological significance.

The CRE dating results from the front of the Fremri-Grjótárdalur rock glacier yielded ages of 6–2 ka (Table 5, Fig. 2, Fig. 8), with two boulders around 6–5 ka. In the view of the results of boulder tracking (Table 1; Tanarro et al., 2019), which point to an evident stagnant state (<0.66 m of horizontal displacement in 14 years), the scatter of ages might be related to the ice melting and subsidence. If we consider that sampled boulders are located in a lower sector of the rock glacier, where the potential ice melting should be higher due to the higher temperature, the probability that a boulder overturned as the ice melted is cannot be ruled out completely. This rock glacier is considered active (Farbrot et al., 2007; Wangensteen et al., 2006; Kellerer-Pirklbauer et al., 2007, Kellerer-Pirklbauer et al., 2008). In a recent study, the mobility of its blocks was restricted to <0.15 m yr^{-1} of horizontal displacement and − 0.37 m in sinking during 14 years (Tanarro et al., 2019). Our results show also limited horizontal movement rates of the boulders. For example, the highest displacement value for a boulder of Hosfdalur debris covered glacier is 5.16 m in 14 years, which means a displacement of 0.37 m yr^{-1}. In the case of

Fremri-Grjótárdalur, the highest displacement value for a block is 2.2 m, that is, 0.16 m yr^{-1} (Table 1). Other authors have obtained higher values in these same rock glaciers, but with automatic digital photogrammetry. Specifically, these authors propose 0.6 m yr^{-1} to 0.74 m yr^{-1} (Kellerer-Pirklbauer et al., 2007) or 0.07 m yr^{-1} to 0.89 m yr^{-1} (Wangensteen et al., 2006). On the contrary, the values obtained in this work are similar to those obtained by direct observation through total station in Nautárdalur rock glacier, also in Tröllaskagi, with values between 0.2 m yr^{-1} to 0.25 m yr^{-1} (Whalley et al., 1995a, Whalley et al., 1995b). Our results would be within the range of rock glaciers of very low activity, for example, among those studied in the Alps, where movements have been measured from a few cm yr^{-1} up to 10 m yr^{-1} (Delaloye et al., 2010). Previous work has shown that the boulders with greatest horizontal displacement in the debris covered glaciers are also those that have had the greatest sinking (Tanarro et al., 2019; Campos et al., 2019). The morphology of these formations has not changed in 50 years, which suggests that the surface of these formations is sinking uniformly. As a consequence of this process and the location of the tracked boulders in a gentle slope, the dynamics observed point to a slight horizontal displacement (Tanarro et al., 2019; Campos et al., 2019). It is important to consider that both rock glaciers and debris covered glaciers are approximately at the limit of permafrost (Wangensteen et al., 2006; Etzelmüller et al., 2007; Czekirda et al., 2019), probably in thermal conditions in which the layer of debris is sufficient to insulate the internal ice from radiation, although in fact there is no accretion of permafrost. In the view of the limited mobility of the active rock glaciers and debris-covered glaciers and their predominant subsidence dynamics, it seems to be evident that they have no longer accumulate ice in their headwall areas (accumulation zone).

Our information obtained about the almost null flow of these formations is limited to the last decades, in agreement with previous works (Tanarro et al., 2019; Campos et al., 2019). This practically null movement occurs while interstitial ice is present inside the studied rock glaciers. In the case of the debris-covered glaciers, the glacial ice is covered by a thin layer of debris, around one meter thick (Farbrot et al., 2007; Kellerer-Pirklbauer et al., 2007; Andrés et al., 2018; Tanarro et al., 2019; Campos et al., 2019). However, despite of this movement, no change in the morphology of both rock glaciers and debris-covered glaciers has been detected in the last fifty years (Tanarro et al., 2019; Campos et al., 2019), except for the formation of thermokarst depressions indicative of a slow ice melting.

We assume that, despite the debris-covered and rock glaciers still contain internal ice, they have had a very limited or almost null flow the last thousands of years, otherwise boulders would have moved and overturned and consequently, their dated surfaces would not have been constantly exposed to cosmic radiation. If these formations had experienced an important flow with boulder toppling, the exposure ages of the sampled boulders would be much younger and less coherent. However, all our dated surfaces are chronologically coherent, except sample FDGsingle bond1B, which is 3–4 ka younger than the two adjacent boulders, probably due to an overturning. These results support that the Hólar debris-covered and rock glaciers have been static for a long period and that consequently, most of the sampled surfaces of their boulders have been continuously exposed to cosmic radiation without disturbances (e.g. overturning) continuously during the last 5 ka. As a suggestion, this date of definitive stabilization could reflect the impact of the Holocene Thermal Maximum (HTM), which in Tröllaskagi entailed the maximum birch expansion between 8 and 5 ka BP, with temperatures higher than at present (1961–

1990 series) (Wastl et al., 2001; Caseldine et al., 2006). According to lake sediment dating, the ice cap Drangajökull glacier, in northeast Iceland, had retreated compared to its current extent (Schomacker et al., 2016) or even disappeared (Harning et al., 2016, Harning et al., 2018) at that time, just as other central ice-caps (Anderson et al., 2018b; Geirsdóttir et al., 2018). A MAAT >3 °C above the present mean value would be required for this to occur (Anderson et al., 2018b; Geirsdóttir et al., 2018). We can therefore deduce that the Fremri-Grjótárdalur rock glacier flow ended during the HTM, when the headland glacier stopped feeding the tongue, composed of a mixture of debris and ice, which remained static, as it was above the permafrost level in this period (Etzelmüller et al., 2007; Wangensteen et al., 2006).

Nevertheless, with our data another interpretation is possible. The present Tröllaskagi rock glaciers with internal ice could have been formed at the onset of the Neoglacial cooling, 5 ka ago (see synthesis in Geirsdóttir et al., 2018). However, more subsurface data of the active rock glaciers (e.g. ice petrography) would be needed to prove the origin of the internal ice: past glaciers or ice formed under permafrost conditions (Ribolini et al., 2007). Moreover, if the origin of interstice ice in the rock glacier had been related to the accretion of ice in permafrost conditions, more time would have been necessary for its formation before its early stabilization.

The comparison of our results with other cases is complicated, since the boulders on the top of an active rock glacier (Fig. 12) have only been dated very rarely, e.g. by Winkler and Lambiel, 2018 (Southern Alps) with the Schmidt-Hammer method, and on the basis of a calibration curve reconstructed with the help of CRE-dated boulders of an adjacent

758 moraine. This work supports our hypothesis according to which the CRE ages from the
759 rock glacier boulders would be indicating the age of the rock glacier stabilization.

760

761 The results obtained in the Hofsjökull debris-covered glacier are similar to those of the
762 stagnant active rock glaciers in Fremri-Grjótárdalur. Three boulders at the glacier front
763 yielded similar ages of 7–5 ka, thus supporting its possible "stabilization" during the
764 HTM. It is important to remember that these blocks belong to a 2 m thick debris cover,
765 resting on about 20 m thick glacial ice. Their current boulder subsidence rate is of
766 −0.55 m yr-1 and the horizontal displacement ranges from 0.18 to 0.37 m yr^{-1}, probably
767 derived from the subsidence processes, and their frontal limits did not advance over the
768 past 50 years.

769

770 The CRE results obtained from the collapsed sector of the Héðinsdalsjökull debris-
771 covered glacier, at 650 m a.s.l., yielded ages between 3 and 2 ka. This front is now
772 completely static and has no internal ice. We assume that these boulders could easily
773 rotate when the glacier ice melted, and therefore their cosmogenic age shows the time
774 that they have been stable since then. CRE dates previously obtained on fossil debris-
775 covered glaciers suggest different durations of existence when these glaciers are exposed
776 to strong solar radiation and thus lost the ice shortly after being formed, compared to
777 nearby glaciers which are more shielded, with glacial activity lasting for thousands of
778 years (Fernández-Fernández et al., 2017a). Thus, our results may show the end of some
779 Neoglacial advances in Tröllaskagi around 3.2 ka (Caseldine and Hatton, 1994; Stötter et
780 al., 1999; Wastl et al., 2001 among others), as it occurred in some sectors of Drangajökull
781 (Harning et al., 2016, Harning et al., 2018), where lake records indicate severe cooling in
782 Iceland (synthesis in Geirsdóttir et al., 2018).

7. Conclusions.

Our results allow a preliminary reconstruction of the glacier behavior in valleys and cirques of the Tröllaskagi peninsula during and after the last deglaciation. The deglaciation of the main valleys (Viðinesdalur and Kolbeinsdalur) in the Tröllaskagi peninsula began their retreat at around 16 ka. The glacier dynamics between the onset of deglaciation and the beginning of the Holocene cannot be determined at present, as in our study area no glacial landforms are preserved between the terminal part of the valleys and the base of the cirques. Small moraines exist in these cirques, with ages apparently corresponding to the last glacial advance in the fjords, probably during the Preboreal, around 11 ka. After this date, the glaciers retreated and temperatures rose abruptly, as in the rest of Iceland, triggering paraglacial processes on the deglaciated walls, including gravitational events, with the subsequent formation of debris-covered and rock glaciers whose fronts shortly after stabilized, especially those at lower altitudes.

New rock glaciers and debris-covered glaciers were then formed at the upper sectors of the valleys sometime after the Preboreal. These new formations still retain currently internal ice covered by debris. Moreover, they display minimal dynamics, mainly related to subsidence. These limited dynamics allowed most of the boulder surfaces resting on the ice to be continuously exposed to cosmic radiation. This indicates that these debris-covered glaciers and rock glaciers no longer accumulated ice in their head areas. This stabilization timing oscillates between 7 and 3 ka ago and may have been caused either by the HTM warm period or remobilization during the cold Neoglacial periods. Thus, this research demonstrates the potential of CRE dating methods in the study of the past dynamics of debris-covered glaciers and rock glaciers both in the frame of the glacial

landscape evolution and in the understanding of the debris-free glaciers transformation to debris-covered and rock glaciers. However, to fully understand this evolution and its origin, more information must be collected both from other nearby rock glaciers or debris-covered glaciers to have a more complete overview and more representative study cases in a statistical point of view. Subsurface data would also have a great potential as internal ice of rock glacier and debris-covered glaciers is not present homogeneously in the detrital bodies, and this information would complement the conclusions derived from the boulder mobility/stability analysis.

Acknowledgements

This paper was funded by the project CGL2015-65813-R (Spanish Ministry of Economy and Competitiveness) and Nils Mobility Program (EEA GRANTS), and with the help of the High Mountain Physical Geography Research Group (Complutense University of Madrid). We thank the Icelandic Association for Search and Rescue, the Icelandic Institute of Natural History, the Hólar University College, and David Palacios Jr. and María Palacios for their support in the field. José M. Fernández-Fernández received a PhD fellowship from the FPU programme (Spanish Ministry of Education, Culture and Sport; reference FPU14/06150). The ^{36}Cl measurements were performed at the ASTER AMS national facility (CEREGE, Aix-en-Provence), which is supported by the INSU/CNRS and the ANR through the "Projets thématiques d'excellence" program for the "Equipements d'excellence" ASTER-CEREGE action and IRD. The authors express their deep gratitude to Dr. Adriano Ribolini and an anonymous reviewer, whose corrections and suggestions have contributed significantly to improve the earlier draft of the manuscript and figures.

References

833 Ackert, jr., R.P., 1998. A rock glacier/debris-covered glacier system at Galena Creek,
834 Absaroka mountains, Wyoming. Geogr. Ann. Ser. A, Phys. Geogr. 80, 267–276.
835 https://doi.org/10.1111/j.0435-3676.1998.00042.x

836 Alley, R.B., Ágústsdóttir, A.M., 2005. The 8k event: Cause and consequences of a major
837 Holocene abrupt climate change. Quat. Sci. Rev. 24, 1123–1149.
838 https://doi.org/10.1016/j.quascirev.2004.12.004

839 Anderson, L.S., Anderson, R.S., 2016. Modeling debris-covered glaciers: response to
840 steady debris deposition. Cryosph. 10, 1105–1124. https://doi.org/10.5194/tc-10-
841 1105-2016

842 Anderson, L.S., Flowers, G.E., Jarosch, A.H., Aðalgeirsdóttir, G.T., Geirsdóttir, Á.,
843 Miller, G.H., Harning, D.J., Thorsteinsson, T., Magnússon, E., Pálsson, F., 2018b.
844 Holocene glacier and climate variations in Vestfirðir, Iceland, from the modeling of
845 Drangajökull ice cap. Quat. Sci. Rev. 190, 39–56.
846 https://doi.org/10.1016/j.quascirev.2018.04.024

847 Anderson, R.S., Anderson, L.S., Armstrong, W.H., Rossi, M.W., Crump, S.E., 2018a.
848 Glaciation of alpine valleys: The glacier–debris-covered glacier–rock glacier
849 continuum. Geomorphology 311, 127-142.
850 https://doi.org/10.1016/j.geomorph.2018.03.015.

851 Andrés, N., Gómez-Ortiz, A.., Fernández-Fernández, J.M., Tanarro, L.M., Salvador-
852 Franch, F., Oliva, M., Palacios, D., 2018a. Timing of deglaciation and rock glacier
853 origin in the southeastern Pyrenees: a review and new data. Boreas.
854 https://doi.org/10.1111/bor.12324

855 Andrés, N., Palacios, D., Saemundsson, Þ., Brynjólfsson, S., Fernández-Fernández, J.M.,
856 2018b. The rapid deglaciation of the Skagafjörður fjord, northern Iceland. Boreas.
857 https://doi.org/10.1111/bor.12341

858 Andrés, N., Tanarro, L.M., Fernández, J.M., Palacios, D., 2016. The origin of glacial
859 alpine landscape in Tröllaskagi Peninsula (North Iceland). Cuad. Investig.
860 Geográfica 42 (2), 341-368. http://dx.doi.org/10.18172/cig.2935.

861 Andrews, J.T., Harðardóttir, J., Helgadóttir, G., Jennings, A.E., Geirsdóttir, Á.,
862 Sveinbjörnsdóttir, Á.E., Schoolfield, S., Kristjánsdóttir, G.B., Smith, L.M., Thors,
863 K., Syvitski, J., 2000. The N and W Iceland Shelf: Insights into Last Glacial
864 Maximum ice extent and deglaciation based on acoustic stratigraphy and basal
865 radiocarbon AMS dates. Quat. Sci. Rev. 19, 619-631. https://doi.org/10.1016/S0277-
866 3791(99)00036-0

867 Azócar, G., Brenning, A., 2010. Hydrological and geomorphological significance of rock
868 glaciers in the dry Andes, Chile (27º-33ºS). Permafr. Periglac. Process. 21 (1), 42-
869 53. http://dx.doi.org/10.1002/ppp.669.

870 Bachrach, T., Jakobsen, K., Kinney, J., Nishimura, P., Reyes, A., Laroque, C.P., Smith,
871 D.J., 2004. Dendrogeomorphological assessment of movement at Hilda rock glacier,
872 Banff National Park, Canadian Rocky Mountains. Geogr. Ann., 86 A (1): 1–9.

873 Ballantyne, C.K., Schnabel, Ch., Xu, S., 2009. Exposure dating and reinterpretation of
874 coarse debris accumulations (‘rock glaciers’) in the Cairngorm Mountains, Scotland.
875 J. Quat. Sci. 24, 19-31. https://doi.org/10.1002/jqs.1189

876 Ballantyne, C.K., 2013. Paraglacial Geomorphology, in: Encyclopedia of Quaternary
877 Science: Second Edition. Elsevier, pp. 553–565. https://doi.org/10.1016/B978-0-
878 444-53643-3.00089-3

879 Barsch, D., 1996. Rock Glaciers. Springer, Berlin, 331 pp.

880 Benedict, J.B. 1973. Chronology cirque glaciation, Colorado Front Range. Quat. Res. 3,
881 584-599. https://doi.org/10.1016/0033-5894(73)90032-X

882 Benn, D.I., Bolch, T., Hands, K., Gulley, J., Luckman, A., Nicholson, L.I., Quincey, D.,
883 Thompson, S., Toumi, R., Wiseman, S., 2012. Response of debris-covered glaciers
884 in the Mount Everest region to recent warming, and implications for outburst flood
885 hazards. Earth-Science Rev. 114, 156–174.
886 https://doi.org/10.1016/j.earscirev.2012.03.008

887 Berger, J., Krainer, K., Mostler, W., 2004. Dynamics of an active rock glacier (Ötztal
888 Alps, Austria). Quat. Res. 62, 233–242.
889 https://doi.org/10.1016/J.YQRES.2004.07.002

890 Bibby, T., Putkonen, J., Morgan, D., Balco, G., Shuster, D.L., 2016. Million year old ice
891 found under meter thick debris layer in Antarctica. Geophys. Res. Lett. 43 (13),
892 6995e7001. http://dx.doi.org/10.1002/2016GL069889.

893 Björnsson, H., Pálsson, F., 2008. Icelandic glaciers. Jökull 58, 365–386.

894 Bosson, J.B., Lambiel, C., 2016. Internal Structure and Current Evolution of Very Small
895 Debris-Covered Glacier Systems Located in Alpine Permafrost Environments. Front.
896 Earth Sci. 4. https://doi.org/10.3389/feart.2016.00039

897 Brenning, A., 2005. Geomorphological, hydrological and climatic significance of rock
898 glaciers in the Andes of Central Chile (33-35°S). Permafr. Periglac. Process. 16, 231–
899 240. https://doi.org/10.1002/ppp.528

Briner, J. P., Tulenko, J. P., Young, N. E., Baichtal, J. F., & Lesnek, A., 2017. The last deglaciation of Alaska. Cuadernos de Investigación Geográfica, 43(2), 429-448. http://dx.doi.org/10.18172/cig.3229

Brynjólfsson, S., Schomacker, A., Ingólfsson, Ó., Keiding, J.K., 2015. Cosmogenic ^{36}Cl exposure ages reveal a 9.3 ka BP glacier advance and the Late Weichselian-Early Holocene glacial history of the Drangajökull region, northwest Iceland. Quat. Sci. Rev. 126, 140–157. doi:10.1016/j.quascirev.2015.09.001

Campos, N., Tanarro, L.M., Palacios, D., Zamorano, J.J., 2019. Slow dynamics in debris-covered and rock glaciers in Hofsdalur, Tröllaskagi Peninsula (northern Iceland). Geomorphology 342, 61–77. https://doi.org/10.1016/j.geomorph.2019.06.005

Capt, M., Bosson, J.B.B., Fischer, M., Micheletti, N., Lambiel, C., 2016. Decadal evolution of a very small heavily debris-covered glacier in an Alpine permafrost environment. J. Glaciol. 62, 535–551. https://doi.org/10.1017/jog.2016.56

Caseldine, C., Hatton, J., 1994. Environmental change in Iceland. Münchener Geogr. Abhandlungen. R. B Bd. B 12 41–62.

Caseldine, C., Langdon, P.G., Holmes, N. 2006. Early Holocene climate variability and the timing and extent of the Holocene thermal maximum (HTM) in northern Iceland. Quat. Sci. Rev. 25, 2314-2331. https://doi.org/10.1016/j.quascirev.2006.02.003

Caseldine, C., Stötter, J., 1993. “Little Ice Age” glaciation of Tröllaskagi peninsula, northern Iceland: climatic implications for reconstructed equilibrium line altitudes (ELAS). The Holocene 3, 357–366. https://doi.org/10.1177/095968369300300408

921 Caseldine, C.J., 1985. The Extent of Some Glaciers in Northern Iceland during the Little
922 Ice Age and the Nature of Recent Deglaciation. Geogr. J. 151, 215–227.
923 https://doi.org/10.2307/633535

924 Çiner, A., Sarikaya, M.A., Yildirim, C., 2017. Misleading old age on a young landform?
925 The dilemma of cosmogenic inheritance in surface exposure dating: Moraines vs.
926 rock glaciers. Quaternary Geochronology 42, 76-88.
927 https://doi.org/10.1016/j.quageo.2017.07.003

928 Clark, D.H., Clark, M.M., Gillespie, A.R., 1994. Debris-covered glaciers in the Sierra
929 Nevada, California, and their implications for snowline reconstructions. Quat. Res.
930 https://doi.org/10.1006/qres.1994.1016

931 Coquin, J., Mercier, D., Bourgeois, O., Cossart, E., Decaulne, A., 2015. Gravitational
932 spreading of mountain ridges coeval with Late Weichselian deglaciation: Impact on
933 glacial landscapes in Tröllaskagi, northern Iceland. Quat. Sci. Rev. 107, 197–213.
934 doi:10.1016/j.quascirev.2014.10.023

935 Cossart, E., Mercier, D., Decaulne, A., Feuillet, T., Jónsson, H.P., Saemundsson, Þ., 2014.
936 Impacts of post-glacial rebound on landslide spatial distribution at a regional scale in
937 northern Iceland (Skagafjörður). Earth Surf. Process. Landforms 39, 336–350.
938 https://doi.org/10.1002/esp.3450

939 Crochet, P., Jóhannesson, T., Jónsson, T., Sigurðsson, O., Björnsson, H., Pálsson, F.,
940 Barstad, I., 2007. Estimating the Spatial Distribution of Precipitation in Iceland
941 Using a Linear Model of Orographic Precipitation. J. Hydrometeorol. 8, 1285–1306.
942 https://doi.org/10.1175/2007JHM795.1

Czekirda, J., Westermann, S., Etzelmüller, B., & Jóhannesson, T. (2019). Transient modelling of permafrost distribution in Iceland. Frontiers in Earth Science, 7, 130. https://doi.org/10.3389/feart.2019.00130

Decaulne, A., Cossart, E., Mercier, D., Feuillet, T., Coquin, J., Jónsson, H.P., 2016. An early Holocene age for the Vatn landslide (Skagafjörður, central northern Iceland): Insights into the role of postglacial landsliding on slope development. The Holocene 26, 1304-1318. https://doi.org/10.1177/0959683616638432

Dede, V., Cicek, I., Sarikaya, M. A., Ciner, A., Uncu, L., 2017. First cosmogenic geochronology from the Lesser Caucasus: late Pleis- tocene glaciation and rock glacier development in the Karçal Valley, NE Turkey. Quat. Sci. Rev. 164, 54–67. https://doi.org/10.1016/j.quascirev.2017.03.025

Delaloye, R., Perruchoud, E., Avian, M., Kaufmann, V., Bodin, X., Hausmann, H., Ikeda, A., Kääb, A., Kellerer-Pirklbauer, A., Krainer, K., Lambiel, C., Mihajlovic, D., Staub, B., Roer, I., Thibert, E., 2008. Recent Inter annual Variations of Rock Glacier Creep in the European Alps, in: Ninth International Conference on Permafrost. Fairbanks, Alaska, United States, pp. 343–348.

Delaloye, R., Lambiel, C. and Gärtner-Roer, I. (2010). Overview of rock glacier kinematics research in the Swiss Alps. Geographica Helvetica, 65 (2): 135- 145.

Deline, P., Akçar, N., Ivy-Ochs, S., Kubik, P.W., 2015. Repeated Holocene rock avalanches onto the Brenva Glacier, Mont Blanc massif, Italy: A chronology. Quat. Sci. Rev. 126, 186-200 http://dx.doi.org/10.1016/j.quascirev.2015.09.004

Emmer, A., Loarte, E.C., Klimeš, J., Vilímek, V., 2015. Recent evolution and degradation of the bent Jatunraju glacier (Cordillera Blanca, Peru). Geomorphology 228, 345–355. https://doi.org/10.1016/J.GEOMORPH.2014.09.018

967 Eriksen, H.Ø., Rouyet, L., Lauknes, T.R., Berthling, I., Isaksen, K., Hindberg, H., Corner,
968 G.D., 2018. Recent Acceleration of a Rock Glacier Complex, Ádjet, Norway,
969 Documented by 62 Years of Remote Sensing Observations. Geophysical Research
970 Letters 45 (16), 8314-8323. https://doi.org/10.1029/2018GL077605

971 Etzelmüller, B., Farbrot, H., Guðmundsson, Á., Humlum, O., Tveito, O.E., Björnsson,
972 H., 2007. The regional distribution of mountain permafrost in Iceland. Permafr.
973 Periglac. Process. 18, 185–199. https://doi.org/10.1002/ppp.583

974 Farbrot, H., Etzelmüller, B., Guðmundsson, Á., Humlum, O., Kellerer-Pirklbauer, A.,
975 Eiken, T., Wangensteen, B., 2007. Rock glaciers and permafrost in Tröllaskagi,
976 northern Iceland. Z. Geomorph. N.F. (Suppl. 51), 1–16.
977 https://doi.org/10.1127/0372-8854/ 2007/0051S2-0001

978 Fernández-Fernández, J.M., Palacios, D., García-Ruiz, J.M., Andrés, N.,
979 Schimmelpfennig, I., Gómez-Villar, A., Santos-González, J., Álvarez-Martínez, J.,
980 Arnáez, J., Úbeda, J., Léanni, L., Aumaître, G., Bourlès, D., Keddadouche, K., 2017a.
981 Chronological and geomorphological investigation of fossil debris-covered glaciers
982 in relation to deglaciation processes: A case study in the Sierra de La Demanda,
983 northern Spain. Quat. Sci. Rev. 170, 232–249.
984 https://doi.org/10.1016/j.quascirev.2017.06.034

985 Fernández-Fernández, J.M., Andrés, N., Sæmundsson, Þ., Brynjólfsson, S., Palacios, D.,
986 2017b. High sensitivity of North Iceland (Tröllaskagi) debris-free glaciers to climatic
987 change from the 'Little Ice Age' to the present. The Holocene 27, 1187–1200.
988 https://doi.org/10.1177/0959683616683262

989 Fernández-Fernández, J.M., Palacios, D., Andrés, N., Schimmelpfennig, I., Brynjólfsson,
990 S., Sancho, L.G., Zamorano, J.J., Heiðmarsson, S., Sæmundsson, Þ., 2019. A multi-

proxy approach to Late Holocene fluctuations of Tungnahryggsjökull glaciers in the Tröllaskagi peninsula (northern Iceland). Sci. Total Environ. 664, 499–517. https://doi.org/10.1016/j.scitotenv.2019.01.364

Feuillet, T., Coquin, J., Mercier, D., Cossart, E., Decaulne, A., Jónsson, H.P., Sæmundsson, Þ., 2014. Focusing on the spatial non-stationarity of landslide predisposing factors in northern Iceland. Prog. Phys. Geogr. 38, 354–377. https://doi.org/10.1177/0309133314528944

Fink, D., Vogt, S., Hotchkis, M., 2000. Cross-sections for ^{36}Cl from Ti at Ep=35–150 MeV: Applications to in-situ exposure dating. Nucl. Instruments Methods Phys. Res. Sect. B Beam Interact. with Mater. Atoms 172, 861–866. doi:10.1016/S0168-583X(00)00200-7

Fuchs, M.C., Bohlert, R., Krbetschek, M., Preusser, F., Egli, M., 2013. Exploring the potential of luminescence methods for dating Alpine rock glaciers. Quat. Geochronol. 18, 17-33. http://dx.doi.org/10.1016/j.quageo.2013.07.001.

Galanin, A.A. Lytkin, V.M. Fedorov, A.N. Kadota, T. 2014, Kriosfera Zemli, XVIII (2), 64–74.

Geirsdóttir, Á., Andrews, J.T., Ólafsdóttir, S., Helgadóttir G., Harðardóttir J., 2002. A 36 Ky record of iceberg rafting and sedimentation from north-west Iceland. Polar Research 21, 291-298. https://doi.org/10.3402/polar.v21i2.6490

Geirsdóttir, Á., Miller, G.H., Andrews, J.T., Harning, D.J., Anderson, L.S., Thordarson, T., 2018. The onset of Neoglaciation in Iceland and the 4.2 ka event. Clim. Past Discuss. 1–33. https://doi.org/10.5194/cp-2018-130

1013 Geirsdóttir, Á., Miller, G.H., Axford, Y., Ólafsdóttir, S., 2009. Holocene and latest
1014 Pleistocene climate and glacier fluctuations in Iceland. Quat. Sci. Rev. 28, 2107–
1015 2118. https://doi.org/10.1016/j.quascirev.2009.03.013

1016 Giardino, J.R., Vitek, J.D., 1988. The significance of rock glaciers in the glacial
1017 periglacial landscape continuum. J. Quat. Sci. 3 (1), 97-103.
1018 http://dx.doi.org/10.1002/jqs.3390030111

1019 Gibson, M.J., Glasser, N.F., Quincey, D.J., Rowan, A.V., Irvine-Fynn, T.D., 2017.
1020 Changes in glacier surface cover on Baltoro glacier, Karakoram, north Pakistan,
1021 2001–2012. J. Maps 13, 100–108. https://doi.org/10.1080/17445647.2016.1264319

1022 Glasser, N.F., Jansson, K.N., Duller, G.A.T., Singarayer, J., Holloway, M., Harrison, S.,
1023 2016. Glacial lake drainage in Patagonia (13–8 kyr) and response of the adjacent
1024 Pacific Ocean. Sci. Rep. 6, 21064.

1025 Haeberli, W., Brandova, D., Burga, C., Egli, M., Frauenfelder, R., Kääb, A., Maisch, M.,
1026 Mauz, B., Dikau, R., 2003. Methods for absolute and relative age dating of
1027 rockglacier surfaces in alpine permafrost. In: Phillips, M., Springman, S., Arenson,
1028 L. (Eds.), Proceedings of the 8th International Conference on Permafrost 2003,
1029 Zürich, pp. 343-348.
1030 http://www.arlis.org/docs/vol1/ICOP/55700698/Pdf/Chapter_062.pdf.

1031 Haeberli, W., Hallet, B., Arenson, L., Elconin, R., Humlum, O., Kääb, A., Kaufmann, V.,
1032 Ladanyi, B., Matsuoka, N., Springman, S., Vonder Mühll, D., 2006. Permafrost creep
1033 and rock glacier dynamics. Permafr. Periglac. Process. 17 (3), 189-214.
1034 http://dx.doi.org/10.1002/ppp.561.

1035 Hambrey, M.J., Quincey, D.J., Glasser, N.F., Reynolds, J.M., Richardson, S.J.,
1036 Clemmens, S., 2008. Sedimentological, geomorphological and dynamic context of

debris-mantled glaciers, Mount Everest (Sagarmatha) region, Nepal. Quat. Sci. Rev. 27, 2361–2389. https://doi.org/10.1016/j.quascirev.2008.08.010

Hamilton, S.J., Whalley, W.B., 1995a. Preliminary results from the lichenometric study of the Nautardalur rock glacier, Tröllaskagi, northern Iceland. Geomorphology 12, 123–132. https://doi.org/10.1016/0169-555X(94)00083-4

Hamilton, S.J., Whalley, W.B., 1995b. Rock glacier nomenclature: a re-assessment. Geomorphology 14, 73–80. https://doi.org/10.1016/0169-555X(95)00036-5.

Harning, D.J., Geirsdóttir, Á., Miller, G.H., Zalzal, K., 2016. Early Holocene deglaciation of Drangajökull, Vestfirðir, Iceland. Quat. Sci. Rev. 153, 192–198. doi:10.1016/j.quascirev.2016.09.030

Harning, D.J., Thordarson, T., Geirsdóttir, Á., Zalzal, K., Miller, G.H., 2018. Provenance, stratigraphy and chronology of Holocene tephra from Vestfirðir, Iceland. Quat. Geochronol. 46, 59–76. https://doi.org/10.1016/J.QUAGEO.2018.03.007

Hippolyte, J.C., Bourlès, D., Braucher, R., Carcaillet, J., Léanni, L., Arnold, M., Aumaitre, G., 2009: Cosmogenic 10Be dating of a sackung and its faulted rock glaciers, in the Alps of Savoy (France). Geomorphology 108, 312-320 http://www.springer.com/us/book/9783642800955.

Hubbard, A., Sugden, D., Dugmore, A., Norddahl, H., Pétursson, H.G., 2006. A modelling insight into the Icelandic Last Glacial Maximum ice sheet. Quat. Sci. Rev. 25, 2283–2296. https://doi.org/10.1016/J.QUASCIREV.2006.04.001

Humlum, O., 1998. The climatic significance of rock glaciers. Permafr. Periglac. Process. 9, 375–395. https://doi.org/10.1002/(SICI)1099-1530(199810/12)9:4<375::AID-PPP301>3.0.CO;2-0

1060 Humlum, O., 2000. The geomorphic significance of rock glaciers: estimates of rock
1061 glacier debris volumes and headwall recession rates in West Greenland.
1062 Geomorphology 35, 41–67. https://doi.org/10.1016/S0169-555X(00)00022-2

1063 Icelandic Meteorological Office, 2018. Climatological data. Available on
1064 http//en.vedur.is/climatology/data/ (accessed 13 April 2018).

1065 Ingólfsson, O., 1991. A review of the late Weichselian and early Holocene glacial and
1066 environmental history of Iceland. In: J. Maizels, C. Caseldine (eds.), Environmental
1067 Change in Iceland: Past and Present, Kluwer Academic Publishers, Dordrecht, pp.
1068 13-29.

1069 Ingólfsson, O., Norðdahl, H., 2001. High Relative Sea Level during the Bolling
1070 Interstadial in Western Iceland: A Reflection of Ice-Sheet Collapse and Extremely
1071 Rapid Glacial Unloading. Arctic, Antarct. Alp. Res. 33, 231.
1072 https://doi.org/10.2307/1552224

1073 Ivy-Ochs, S., Synal, H.-A., Roth, C., Schaller, M., 2004. Initial results from isotope
1074 dilution for Cl and ^{36}Cl measurements at the PSI/ETH Zurich AMS facility. Nucl.
1075 Instruments Methods Phys. Res. Sect. B Beam Interact. with Mater. Atoms 223–224,
1076 623–627. https://doi.org/10.1016/j.nimb.2004.04.115

1077 Janke, J.R., Bellisario, A.C., Ferrando, F.A., 2015. Classification of debris-covered
1078 glaciers and rock glaciers in the Andes of central Chile. Geomorphology 241, 98-
1079 121. http://dx.doi.org/10.1016/j.geomorph.2015.03.034

1080 Janke, J.R., Regmi, N.R., Giardino, J.R., Vitek, J.D., 2013. 8.17 Rock glaciers. In:
1081 Shroder, J. (Ed.), Treatise in Geomorphology, Volume 8. Elsevier, pp. 238-273.
1082 https://www.researchgate.net/publication/237102263_Rock_Glacier.

Johnson, P.G., 1980. Rock glaciers: glacial and non-glacial origins. World Glacier Inventory - inventaire mondial des Glaciers. In: (Proceedings of the Riederalp Workshop, September 1978: Actes de l'Atelier de Riederalp, septembre 1978), vol. 126. International Association of Scientific Hydrology, pp. 285e293. http://hydrologie.org/redbooks/a126/iahs_126_0285.pdf.

Jones, D.B., Harrison, S., Anderson, K., Selley, H.L., Wood, J.L., Betts, R.A., 2018. The distribution and hydrological significance of rock glaciers in the Nepalese Himalaya. Glob. Planet. Change 160, 123–142. https://doi.org/10.1016/J.GLOPLACHA.2017.11.005

Jónsson, O., 1976. Berghlaup. Ræktunarfélag Norðurlands, Akureyri.

Kaldal, I., Víkingsson, S. 1990. Early Holocene deglaciation in Central Iceland. Jökull 40, 51-66.

Kellerer-Pirklbauer, A., 2012. The Schmidt-Hammer as a Relative Age Dating Tool for Rock Glacier Surfaces. Quat. Int. 279–280, 239. https://doi.org/10.1016/J.QUAINT.2012.08.546

Kellerer-Pirklbauer, A., Kaufmann, V., 2012. About the relationship between rock glacier velocity and climate parameters in central Austria. Austrian J. Earth Sci. 105, 94–112.

Kellerer-Pirklbauer, A., Lieb, G.K., Avian, M., G., J., 2008. The response of partially debris-covered valley glaciers to climate change: the example of the Pasterze glacier (Austria) in the period 1964 to 2006. Geogr. Ann. Ser. A, Phys. Geogr. 90, 269–285. https://doi.org/10.1111/j.1468-0459.2008.00345.x

1105 Kellerer-Pirklbauer, A., Lieb, G.K., Kaufmann, V., 2017. The Dösen Rock Glacier in
1106 Central Austria: A key site for multidisciplinary long-term rock glacier monitoring
1107 in the Eastern Alps. Austrian J. Earth Sci. 110.
1108 https://doi.org/10.17738/ajes.2017.0013

1109 Kellerer-Pirklbauer, A., Wangensteen, B., Farbrot, H., Etzelmüller, B., 2007. Relative
1110 surface age-dating of rock glacier systems near Hólar in Hjaltadalur, northern
1111 Iceland. J. Quat. Sci. 23, 137–151. https://doi.org/10.1002/jqs.1117

1112 Kenner, R., 2018. Geomorphological analysis on the interaction of Alpine glaciers and
1113 rock glaciers since the Little Ice Age. L. Degrad. Dev.
1114 https://doi.org/10.1002/ldr.3238

1115 Kenner, R., Phillips, M., Limpach, P., Beutel, J., Hiller, M., 2018. Monitoring mass
1116 movements using georeferenced time-lapse photography: Ritigraben rock glacier,
1117 western Swiss Alps. Cold Regions Science and Technology 145, 127–134.

1118 Kirkbride, M.P., 2000. Ice-marginal geomorphology and Holocene expansion of debris-
1119 covered Tasman glacier, New Zealand. In: Nakawo, M., Raymond, C.F., Fountain,
1120 A. (Eds.), Debris-covered Glaciers, vol. 264. IAHS, pp. 211-217.
1121 http://hydrologie.org/redbooks/a264/iahs_264_0211.pdf.

1122 Kirkbride, M.P., 2011. Debris-covered glaciers. In: Singh, V.P., Singh, P., Haritashya,
1123 U.K. (Eds.), Encyclopedia of Snow, Ice and Glaciers: Encyclopedia of Earth Series.
1124 Springer, Netherlands, pp. 180–182. https://doi.org/10.1007/978-90-481-2642-
1125 2_622

1126 Knight, J., Harrison, S., Jones, D.B., 2018. Rock glaciers and the geomorphological
1127 evolution of deglacierizing mountains. Geomorphology 311, 127–142.
1128 https://doi.org/10.1016/j.geomorph.2018.09.020

Konrad, S.K., Clark, D.C. 1998. Evidence for an Early Neoglacial Glacier Advance from Rock Glaciers and Lake Sediments in the Sierra Nevada, California, U.S.A. Arctic and Alpine Research 30 (3), 272-284. http://www.jstor.org/stable/1551975

Larsen, D.J., Miller, G.H., Geirsdóttir, Á., Ólafsdóttir, S., 2012. Non-linear Holocene climate evolution in the North Atlantic: A high-resolution, multi-proxy record of glacier activity and environmental change from Hvítárvatn, central Iceland. Quat. Sci. Rev. 39, 14–25. https://doi.org/10.1016/j.quascirev.2012.02.006

Leonard, E. M., Laabs, B. J. B., Schweinsberg, A. D., Russell, C. M., Briner, J. P., & Young, N. E. (2017). Deglaciation of the Colorado Rocky Mountains following the Last Glacial Maximum. Cuadernos de Investigación Geográfica, 43(2), 497-526. http://dx.doi.org/10.18172/cig.3234

Li, Y.K., 2018. Determining topographic shielding from digital elevation models for cosmogenic nuclide analysis: a GIS model for discrete sample sites. Journal of Mountain Science 15(5), 939-947. https://doi.org/10.1007/s11629-018-4895-4

Licciardi, J.M., Denoncourt, C.L., Finkel, R.C., 2008. Cosmogenic ^{36}Cl production rates from Ca spallation in Iceland. Earth Planet. Sci. Lett. 267, 365–377. https://doi.org/10.1016/j.epsl.2007.11.036

Licciardi, J.M., Kurz, M.D., Curtice, J.M., 2006. Cosmogenic 3He production rates from Holocene lava flows in Iceland. Earth Planet. Sci. Lett. 246, 251–264. https://doi.org/10.1016/j.epsl.2006.03.016

Licciardi, J.M., Kurz, M.D., Curtice, J.M., 2007. Glacial and volcanic history of Icelandic table mountains from cosmogenic 3He exposure ages. Quat. Sci. Rev. 26, 1529–1546. https://doi.org/10.1016/j.quascirev.2007.02.016

1152 Licciardi, J. M., and Pierce, K. L, 2018. History and dynamics of the Greater Yellowstone
1153 Glacial System during the last two glaciations. Quaternary Science Reviews, 200, 1-
1154 33. https://doi.org/10.1016/j.quascirev.2018.08.027

1155 Lilleøren, K.S., Etzelmüller, B., Gärtner-Roer, I., Kääb, A., Westermann, S.,
1156 Gumundsson, Á., 2013. The Distribution, Thermal Characteristics and Dynamics of
1157 Permafrost in Tröllaskagi, Northern Iceland, as Inferred from the Distribution of
1158 Rock Glaciers and Ice-Cored Moraines. Permafr. Periglac. Process. 24, 322–335.
1159 https://doi.org/10.1002/ppp.1792

1160 Lippl, S., Vijay, S., Braun, M., 2018. Automatic delineation of debris-covered glaciers
1161 using InSAR coherence derived from X-, C-and L-band radar data: a case study of
1162 Yazgyl Glacier. Journal of Glaciology, 1-11. https://doi.org/10.1017/jog.2018.70

1163 Mackay, S.L., Marchant, D.R., 2016. Dating buried glacier ice using cosmogenic 3He in
1164 surface clasts: Theory and application to Mullins Glacier, Antarctica. Quat. Sci. Rev.
1165 140, 75-100. https://doi.org/10.1016/j.quascirev.2016.03.013

1166 Marrero, S.M., Phillips, F.M., Caffee, M.W., Gosse, J.C., 2016. CRONUS-Earth
1167 cosmogenic ^{36}Cl calibration. Quat. Geochronol. 31, 199–219.
1168 https://doi.org/10.1016/j.quageo.2015.10.002

1169 Martin, H.E., Whalley, B., Orr, J., Caseldine, C., 1994. Dating and interpretation of rock
1170 glaciers using lichenometry, south Tröllaskagi, North Iceland. Münchener Geogr.
1171 Arb. 12, 205–224.

1172 Matthews, J.M., Nesje, A., Linge, H., 2013. Relict talus-foot rock glaciers at Øyberget,
1173 upper Ottadalen, Southern Norway: Schmidt hammer exposure ages and
1174 palaeoenvironmental implications. Permafr. Periglac. Process. 24 (4), 336-346.
1175 http://dx.doi.org/10.1002/ppp.1794.

1176 Mayr, E., Hagg, W., 2019. Debris-Covered Glaciers. In T. Heckmann and D. Morche
1177 (eds.), Geomorphology of Proglacial Systems, Geography of the Physical
1178 Environment, pp. 59-71. https://doi.org/10.1007/978-3-319-94184-4_4

1179 Mercier, D., 2008. Paraglacial and paraperiglacial landsystems; concepts, temporal scales
1180 and spatial distribution. Géomorphologie, Relief, Processus, Environnement 14, 223-
1181 233.

1182 Mercier, D., Coquin, J., Feuillet, T., Decaulne, A., Cossart, E., Jónsson, H.P.,
1183 Sæmundsson, Þ., 2017. Are Icelandic rock-slope failures paraglacial? Age evaluation
1184 of seventeen rock-slope failures in the Skagafjörður area, based on geomorphological
1185 stacking, radiocarbon dating and tephrochronology. Geomorphology 296, 45–58.
1186 https://doi.org/10.1016/j.geomorph.2017.08.011

1187 Mercier, D., Cossart, E., Decaulne, A., Feuillet, T., Jónsson, H.P., Sæmundsson, Þ., 2013.
1188 The Höfðahólar rock avalanche (sturzström): chronological constraint of paraglacial
1189 landsliding on an Icelandic hillslope. The Holocene 23, 432–446.
1190 https://doi.org/10.1177/0959683612463104

1191 Monnier, S., Kinnard, C., 2015. Reconsidering the glacier to rock glacier transformation
1192 problem: new insights from the central Andes of Chile. Geomorphology 238, 47-55.
1193 http://dx.doi.org/10.1016/j.geomorph.2015.02.025

1194 Moran, A.P., Ivy-Ochs, S., Vockenhuber, C., Kerschner, H., 2016. Rock Glacier
1195 development in the Northern Calcareous Alps at the Pleistocene-Holocene boundary.
1196 Geomorphology 273, 178-188. https://doi.org/10.1016/j.geomorph.2016.08.017

1197 Norðdahl, H., 1991a. Late Weichselian and early Holocene deglaciation history of
1198 Iceland. Jökull 40, 27-50.

Norðdahl, H., 1991b. A review of the glaciation maximum concept and the deglaciation of Eyjafjörður, North Iceland. In: J. Maizels, C. Caseldine (eds.), Environmental Changes in Iceland: Past and Present, Kluwer Academic Publishers, Dordrecht, pp. 31-47.

Norðdahl, H., Einarsson, T., 2001. Concurrent changes of relative sea-level and glacier extent at the Weichselian–Holocene boundary in Berufjörður, Eastern Iceland. Quat. Sci. Rev. 20, 1607–1622. https://doi.org/10.1016/S0277-3791(01)00006-3

Norðdahl, H., Ingólfsson, Ó., 2015. Collapse of the Icelandic ice sheet controlled by sea-level rise? Arktos 1, 13. https://doi.org/10.1007/s41063-015-0020-x

Norðdahl, H., Pétursson, H. G., 2005. Relative sea level changes in Iceland. New aspects of the Weichselian deglaciation of Iceland. In Caseldine, C., Russel, A., Harðardóttir, J., Knudsen, O. (eds.): Iceland - Modern Processes and Past Environments, 25–78. Elsevier, Amsterdam.

Norðdahl, H., Ingólfsson, O., Pétursson, H.G. Hallsdóttir, M., 2008. Late Weichselian and Holocene environmental history of Iceland. Jökull 58, 343–364.

Oliva, M., Serrano, E., Gómez-Ortiz, A., González-Amuchástegui, M. J., Nieuwendam, A.; Palacios, D., Pérez-Alberti, A., Pellitero, R., Ruiz-Fernández, J., Valcárcel, M., Vieira, G., Antoniades, D., 2016. Spatial and temporal variability of periglaciation of the Iberian Peninsula. Quaternary Science Reviews 137, 176-199. https://doi.org/10.1016/j.quascirev.2016.02.017

Paasche, Ø., Olaf Dahl, S., Bakke, J., Løvlie, R., Nesje, A., 2007. Cirque glacier activity in arctic Norway during the last deglaciation. Quat. Res. 68, 387–399. https://doi.org/10.1016/J.YQRES.2007.07.006

1222 Palacios, D., Andrés, N., García-Ruiz, J. M., Schimmelpfennig, I., Campos, N., Léanni,
1223 L., Aster Team, 2017. Deglaciation in the central Pyrenees during the Pleistocene–
1224 Holocene transition: timing and geomorphological significance. Quat. Sci. Rev. 150,
1225 110-129.

1226 Palacios, D., Andrés, N., López-Moreno, J.I., García-Ruiz, J.M., 2015b. Late Pleistocene
1227 deglaciation in the upper Gállego valley, central Pyrenees. Quat. Res. 83, 397-414.
1228 https://doi.org/10.1016/j.yqres.2015.01.010

1229 Palacios, D., Andrés, N., Marcos, J., Vázquez-Selem, L., 2012. Glacial landforms and
1230 their paleoclimatic significance in Sierra de Guadarrama, central Iberian Peninsula.
1231 Geomorphology 139-140, 67-78. https://doi.org/10.1016/j.geomorph.2011.10.003

1232 Palacios, D., Gómez-Ortiz, A., Andrés, N., Salvador-Franch, F., Oliva, M., 2016. Timing
1233 and new geomorphologic evidence of the last deglaciation stages in Sierra Nevada
1234 (southern Spain). Quat. Sci. Rev. 150, 110-129.
1235 https://doi.org/10.1016/j.quascirev.2016.08.012

1236 Palacios, D., Gómez-Ortiz, A., Andrés, N., Vázquez-Selem, L., Salvador-Franch, F.,
1237 Oliva, M., 2015a. Maximum extent of Late Pleistocene glaciers and last deglaciation
1238 of La Cerdanya mountains, southeastern Pyrenees. Geomorphology 231, 116-129.
1239 https://doi.org/10.1016/j.geomorph.2014.10.037

1240 Patton, H., Hubbard, A., Bradwell, T., Schomacker, A., 2017. The configuration,
1241 sensitivity and rapid retreat of the Late Weichselian Icelandic ice sheet. Earth-
1242 Science Rev. 166, 223–245. https://doi.org/10.1016/J.EARSCIREV.2017.02.001

1243 Pelto, M., Capps, D., Clague, J.J., Pelto, B., 2013. Rising ELA and expanding proglacial
1244 lakes indicate impending rapid retreat of Brady Glacier, Alaska. Hydrol. Process. 27,
1245 3075–3082. https://doi.org/10.1002/hyp.9913.

1246 Pétursson, H.G., Norðdahl, H., Ingólfsson, Ó., 2015. Late Weichselian history of relative
1247 sea level changes in Iceland during a collapse and subsequent retreat of marine based
1248 ice sheet. Cuad. Investig. Geográfica 41, 261. https://doi.org/10.18172/cig.2741

1249 Phillips, F.M., 2003. Cosmogenic ^{36}Cl ages of Quaternary basalt flows in the Mojave
1250 Desert, California, USA. Geomorphology 53, 199–208.
1251 http://dx.doi.org/10.1016/S0169-555X(02)00328-8.

1252 Phillips, F. M., 2016. Cosmogenic nuclide data sets from the Sierra Nevada, California,
1253 for assessment of nuclide production models: I. Late Pleistocene glacial chronology.
1254 Quaternary Geochronology, 35, 119-129.
1255 https://doi.org/10.1016/j.quageo.2015.12.003

1256 Potter, N.J., Steig, E.J., Clark, D.H., Speece, M.A., Clark, G.M., Updike, A.B., 1998.
1257 Galena Creek rock glacier revisited—new observations on an old controversy.
1258 Geogr. Ann. Ser. A, Phys. Geogr. 80, 251–265. https://doi.org/10.1111/j.0435-
1259 3676.1998.00041.x.

1260 Principato, S.M., Geirsdóttir, Á., Jóhannsdóttir, G.E., Andrews, J.T., 2006. Late
1261 Quaternary glacial and deglacial history of eastern Vestfirðir, Iceland using
1262 cosmogenic isotope (^{36}Cl) exposure ages and marine cores. J. Quat. Sci. 21, 271–
1263 285. http://dx.doi.org/10.1002/jqs.978

1264 Rangecroft, S., Harrison, S., Anderson, K., 2015. Rock glaciers as water stores in the
1265 Bolivian Andes: an assessment of their hydrological importance. Arctic, Antarctic,
1266 and alpine research, 47(1), 89-98. https://doi.org/10.1657/AAAR0014-029

1267 Ribolini, A., Chelli, A., Guglielmin, M., Pappalardo, M., 2007. Relationships between
1268 glacier and rock glacier in the Maritime Alps, Schiantala Valley, Italy. Quat. Res. 68,
1269 353–363. https://doi.org/10.1016/j.yqres.2007.08.004

Rodríguez-Rodríguez, L., Jiménez-Sánchez, M., Domínguez-Cuesta, M.J., Rinterknecht, V., Pallàs, R., Aster Team, 2017. Timing of last deglaciation in the Cantabrian Mountains (Iberian Peninsula; North Atlantic region) based on in situ-produced 10Be exposure dating. Quat. Sci. Rev. 171, 166-181. https://doi.org/10.1016/j.quascirev.2017.07.012

Rosenwinkel, S., Korup, O., Landgraf, A., Dzhumabaeva, A., 2015. Limits to lichenometry. Quat. Sci. Rev. 129, 229-238. http://dx.doi.org/10.1016/j.quascirev.2015.10.031.

Rundgren, M., 1995. Biostratigraphic Evidence of the Allerød-Younger Dryas-Preboreal Oscillation in Northern Iceland. Quat. Res. 44, 405–416. https://doi.org/10.1006/QRES.1995.1085

Rundgren, M., Ingólfsson, Ó. 1999. Plant survival in Iceland during periods of glaciations. Journal of Biogeography 26, 387-396.

Sæmundsson, K., Kristjansson, L., McDougall, I., Watkins, N.D., 1980. K-Ar dating, geological and paleomagnetic study of a 5-km lava succession in northern Iceland. J. Geophys. Res. Solid Earth 85, 3628–3646. https://doi.org/10.1029/JB085iB07p03628

Sæmundsson, Þ., Morino, C., Helgason, J. K., Conway, S. J., & Pétursson, H. G. (2018). The triggering factors of the Móafellshyrna debris slide in northern Iceland: Intense precipitation, earthquake activity and thawing of mountain permafrost. Science of the total environment, 621, 1163-1175.

Scapozza, C., Lambiel, C., Bozzini, C., Mari, S., Conedera, M., 2014. Assessing the rock glacier kinematics on three different timescales: A case study from the southern

Swiss Alps. Earth Surf. Process. Landforms 39, 2056–2069. https://doi.org/10.1002/esp.3599

Schimmelpfennig, I., 2009. Cosmogenic ^{36}Cl in Ca and K rich minerals: analytical developments, production rate calibrations and cross calibration with 3He and 21Ne. Doctor Thesis, Universite Paul Cezanne Aix-Marseille III, CEREGE, 324 pp.

Schimmelpfennig, I., Benedetti, L., Finkel, R., Pik, R., Blard, P.H., Bourlès, D., Burnard, P., Williams, A., 2009. Sources of in-situ^{36}Cl in basaltic rocks. Implications for calibration of production rates. Quat. Geochronol. 4, 441–461. https://doi.org/10.1016/j.quageo.2009.06.003

Schimmelpfennig, I., Benedetti, L., Garreta, V., Pik, R., Blard, P.H., Burnard, P., Bourlès, D., Finkel, R., Ammon, K., Dunai, T., 2011. Calibration of cosmogenic ^{36}Cl production rates from Ca and K spallation in lava flows from Mt. Etna (38°N, Italy) and Payun Matru (36°S, Argentina). Geochim. Cosmochim. Acta 75, 2611–2632. https://doi.org/10.1016/j.gca.2011.02.013

Schimmelpfennig, I., Schaefer, J.M., Putnam, A.E., Koffman, T., Benedetti, L., Ivy-Ochs, S., Team, A., Schlüchter, C., 2014. ^{36} l production rate from K-spallation in the European Alps (Chironico landslide, Switzerland). J. Quat. Sci. 29, 407–413. https://doi.org/10.1002/jqs.2720

Schomacker, A., Brynjólfsson, S., Andreassen, J.M., Gudmundsdóttir, E.R., Olsen, J., Odgaard, B. V., Håkansson, L., Ingólfsson, Ó., Larsen, N.K., 2016. The Drangajökull ice cap, northwest Iceland, persisted into the early-mid Holocene. Quat. Sci. Rev. 148, 68–84. https://doi.org/10.1016/J.QUASCIREV.2016.07.007

Sigurðsson, O., Williams, R.S., 2008. Geographic names of Icelandic glaciers: historic and modern. US Geological Survey Professional Paper 1746.

1317 Stone, J.O., 2000. Air pressure and cosmogenic isotope production. J. Geophys. Res.
1318 Solid Earth 105, 23753–23759. https://doi.org/10.1029/2000JB900181

1319 Stone, J.O., Fifielde, K., Vasconcelos, P., 2005. Terrestrial chlorine-36 production from
1320 spallation of iron, in: Abstract of 10th International Conference on Accelerator Mass
1321 Spectrometry. Berkeley, CA.

1322 Stötter, J., Wastl, M., Caseldine, C., Häberle, T., 1999. Holocene palaeoclimatic
1323 reconstruction in northern Iceland: Approaches and results. Quat. Sci. Rev. 18, 457–
1324 474. https://doi.org/10.1016/S0277-3791(98)00029-8

1325 Swanson, T.W., Caffee, M.L., 2001. Determination of ^{36}Cl production rates derived from
1326 the well-dated deglaciation surfaces of Whidbey and Fidalgo Islands, Washington.
1327 Quat. Res. 56, 366–382. https://doi.org/10.1006/qres.2001.2278

1328 Tanarro, L.M., Palacios, D., Andrés, N., Fernández-Fernández, J.M., Zamorano, J.J.,
1329 Sæmundsson, Þ., Brynjólfsson, S., 2019. Unchanged surface morphology in debris-
1330 covered glaciers and rock glaciers in Tröllaskagi peninsula (northern Iceland). Sci.
1331 Total Environ. 648, 218–235. https://doi.org/10.1016/j.scitotenv.2018.07.460

1332 Tanarro, L.M., Palacios, D., Zamorano, J.J., Andrés, N., 2018. Proposal for
1333 geomorphological mapping of debris-covered and rock glaciers and its application to
1334 Tröllaskagi Peninsula (Northern Iceland). J. Maps 14, 692–703.
1335 https://doi.org/10.1080/17445647.2018.1539417

1336 Vázquez-Selem, L., & Lachniet, M. S., 2017. The deglaciation of the mountains of
1337 Mexico and Central America. Cuadernos de Investigación Geográfica, 43(2), 553-
1338 570. http://dx.doi.org/10.18172/cig.3238

1339 Wangensteen, B., Gudmundsson, Á., Eiken, T., Kääb, A., Farbrot, H., Etzelmüller, B.,
1340 2006. Surface displacements and surface age estimates for creeping slope landforms
1341 in Northern and Eastern Iceland using digital photogrammetry. Geomorphology 80,
1342 59–79. https://doi.org/10.1016/j.geomorph.2006.01.034

1343 Wastl, M., Stotter, J., Caseldine, C., 2001. Reconstruction of Holocene Variations of the
1344 Upper Limit of Tree or Shrub Birch Growth in Northern Iceland Based on Evidence
1345 from Vesturardalur-Skíðadalur, Tröllaskagi. Arctic, Antarct. Alp. Res. 33, 191.
1346 https://doi.org/10.2307/1552220

1347 Whalley, W.B., Douglas, G.R., Jonsson, A., 1983. The Magnitude and Frequency of
1348 Large Rockslides in Iceland in the Postglacial. Geogr. Ann. Ser. A, Phys. Geogr. 65,
1349 99–110. https://doi.org/10.2307/520724

1350 Whalley, W.B., Hamilton, S., Palmer, C., Gordon, J., Martin, H.E., 1995. The dynamics
1351 of rock glaciers: data from Tröllaskagi, North Iceland. In: Slaymaker, O. (Ed.),
1352 Steepland Geomorphology. John Wiley & Sons, pp. 129–145.

1353 Whalley, W.B., Palmer, C.F., Hamilton, S.J., Martin, H.E., 1995. An Assessment of Rock
1354 Glacier Sliding Using Seventeen Years of Velocity Data: Nautárdalur Rock Glacier,
1355 North Iceland. Arct. Alp. Res. 27, 345–351. https://doi.org/10.2307/1552027

1356 Winkler, S., Lambiel, C., 2018. Age constraints of rock glaciers in the Southern Alps/New
1357 Zealand – Exploring their palaeoclimatic potential. Holocene 28, 778–790.
1358 https://doi.org/10.1177/0959683618756802

1359 Wirz, V., Gruber, S., Purves, R.S., Beutel, J., Gärtner-Roer, I., Gubler, S., Vieli, A., 2016.
1360 Short-term velocity variations at three rock glaciers and their relationship with
1361 meteorological conditions. Earth Surf. Dyn. 4, 103–123.
1362 https://doi.org/10.5194/esurf-4-103-2016

Xiao, X., Zhao, M., Knudsen, K.L., Sha, L., Eiríksson, J., Gudmundsdóttir, E., Jiang, H., Guo, Z., 2017. Deglacial and Holocene sea–ice variability north of Iceland and response to ocean circulation changes. Earth Planet. Sci. Lett. 472, 14–24. https://doi.org/10.1016/J.EPSL.2017.05.006

Zreda, M., England, J., Phillips, F., Elmore, D., Sharma, P., 1999. Unblocking of the Nares Strait by Greenland and Ellesmere icesheet retreat 10,000 years ago. Nature 398, 139–142. http://dx.doi.org/10.1038/18197

1371 Table 1. Inventory of the photogrammetry-tracked boulders surveyed in the different geomorphological units their mobility measurements for the
1372 1980–1994 period. Note that the low mobility figures pose the sampled boulders as highly reliable.

Geomorphological units	**CRE sample**	**Analized boulders**	**Year 1980**			**Year 1994**			**1980-1994 period**			
			X (m)	Y (m)	Elevation (m a.s.l.)	X (m)	Y (m)	Elevation (m a.s.l.)	Horizontal displacement		Elevation changes	
									Absolute (m 14 yr^{-1})	Velocity (m yr^{-1})	Absolute (m 14 yr^{-1})	Velocity (m yr^{-1})
Moraine boulders at Hóladalsjökull cirque	HOL-1	B-1	501384.27	581422.77	835.36	501384.99	581422.70	835.32	0.723	0.052	-0.04	-0.003
	HOL-2	B-2	501393.24	581350.79	839.98	501392.94	581350.62	840.04	0.345	0.025	0.06	0.004
Moraine boulders at Fremri-Grjótárdalur cirque	FDG-11	B-4	499246.73	580783.27	897.57	499247.03	580781.79	897.53	1.510	0.108	-0.04	-0.003
		B-5	499248.00	580769.41	898.00	499247.80	580768.72	897.93	0.718	0.051	-0.07	-0.005
		B-6	499266.84	580740.85	899.42	499267.27	580740.50	899.74	0.554	0.040	0.32	0.023
Frontal ridge at Fremri-Grjótárdalur western fossil rock glacier	FDG-1, FDG-2	B-7	498805.31	580940.54	871.31	498804.97	580940.22	871.04	0.467	0.033	-0.27	-0.019
		B-8	498828.64	580944.99	866.63	498828.92	580944.85	866.20	0.313	0.022	-0.43	-0.031
		B-9	498871.17	580933.82	867.89	498871.83	580933.79	867.78	0.661	0.047	-0.11	-0.008
Transverse ridge at upper lobe of Fremri-Grjótárdalur western rock glacier with internal ice	FGD-1B, FGD-2B, FGD-3B	B-10	499163.16	580369.13	950.27	499161.8	580370.94	950.20	2.264	0.162	-0.07	-0.005
		B-11	499153.50	580345.39	951.61	499153.30	580347.20	951.57	1.821	0.130	-0.04	-0.003
		B-12	499172.04	580338.82	953.45	499171.96	580340.40	953.62	1.582	0.113	0.17	0.012
		B-13	499221.77	580333.74	952.24	499221.59	580334.79	952.16	1.065	0.076	-0.08	-0.006
		B-14	499153.33	580314.13	956.72	499152.87	580315.89	956.53	1.819	0.130	-0.19	-0.014
Frontal ridge at Fremri-Grjótárdalur eastern fossil rock glacier	FGD-4B, FGD-5B	B-15	499645.82	580131.39	989.73	499645.73	580131.51	989.76	0.150	0.011	0.03	0.002
		B-16	499659.70	580127.30	993.74	499659.43	580127.46	993.38	0.314	0.022	-0.36	-0.026
		B-17	499651.98	580097.27	992.21	499651.94	580097.29	992.00	0.045	0.003	-0.21	-0.015
Frontal ridges at Hosfdalur debris-covered glacier	HOFS-1, HOFS-2, HOFS-3	B-18	502428.88	575959.77	887.63	502424.46	575959.28	887.04	4.447	0.318	-0.59	-0.042
		B-19	502393.88	575939.80	884.95	502390.67	575943.19	883.69	4.669	0.333	-1.26	-0.090
		B-20	502400.52	575931.57	887.51	502396.74	575934.19	886.48	4.599	0.329	-1.03	-0.074
		B-21	502411.46	575920.45	891.44	502407.88	575923.78	890.89	4.889	0.349	-0.55	-0.039
		B-22	502413.24	575917.63	892.38	502409.12	575920.74	891.60	5.162	0.369	-0.78	-0.056
		B-23	502416.01	575675.23	926.16	502412.97	575677.98	925.85	4.099	0.293	-0.31	-0.022
		B-24	502382.18	575667.46	923.25	502379.86	575669.72	923.06	3.239	0.231	-0.19	-0.014
		B-25	502408.02	575627.08	933.75	502406.13	575628.55	933.42	2.394	0.171	-0.33	-0.024
		B-26	502400.35	575616.67	934.97	502398.34	575618.54	934.54	2.745	0.196	-0.43	-0.031
		B-27	502425.77	575603.09	940.43	502423.72	575604.54	940.39	2.511	0.179	-0.04	-0.003

1373

1374 Table 2. Geographic sample locations, topographic shielding factor, sample thickness and distance from headwall.

Sample name	Sample type	Latitude (ºN)	Longitude (ºW)	Elevation (m a.s.l.)	Shielding factor	Thickness (cm)	Distance from the headwall (m)
Glacially polished ridge Elliði							
ELLID-1	Polished bedrock	65.7580	19.0848	597	0.9986	2.0	16000
ELLID-2	Polished bedrock	65.7579	19.0854	597	0.9994	3.5	15900
Moraine boulders of Hóladalur							
HOL-1	Moraine boulder	65.7303	18.9698	833	0.9629	3.0	3400
HOL-2	Moraine boulder	65.7297	18.9696	841	0.9931	3.0	3480
Fremri-Grjótárdalur rock glacier complex							
FGD-1	Rock glacier (inactive) boulder	65.7259	19.0245	869	0.8889	4.0	1480
FGD-2	Rock glacier (inactive) boulder	65.8003	19.0200	874	0.9765	4.5	1640
FGD-11	Moraine boulder	65.7242	19.0159	912	0.9843	5.0	1680
FGD-1B	Rock glacier (active) boulder	65.7207	19.0172	960	0.9932	2.0	1030
FGD-2B	Rock glacier (active) boulder	65.7209	19.0186	960	0.9741	4.0	1080
FGD-3B	Rock glacier (active) boulder	65.7205	19.0186	966	0.9929	3.5	1035
FGD-4B	Rock glacier (inactive) boulder	65.7184	19.0079	1005	0.9841	3.5	830
FGD-5B	Rock glacier (inactive) boulder	65.7187	19.0073	1030	0.9880	4.0	780
Hofsjökull debris-covered glacier							
HOFS-1	Debris-covered glacier (active) boulder	65.6812	18.9481	893	0.9758	2.5	2950
HOFS-2	Debris-covered glacier (active) boulder	65.6811	18.9478	894	0.9557	4.0	2920
HOFS-3	Debris-covered glacier (active) boulder	65.6811	18.9479	903	0.9856	3.5	2930
Héðinsdalsjökull debris-covered glacier							
HEDIN-1	Moraine boulder	65.6454	18.9292	640	0.9758	3.5	4690
HEDIN-2	Moraine boulder	65.6455	18.9272	660	0.9764	2.0	4580
HEDIN-3	Moraine boulder	65.6455	18.9278	653	0.9775	2.5	4610

1375

1376

Table 3. Concentrations of the ^{36}Cl target elements Ca, K, Ti and Fe Ca, K, Ti and Fe, determined in splits taken after the chemical pre-treatment (acid etching).

Sample name	**CaO (%)**	**K_2O (%)**	**TiO_2 (%)**	**Fe_2O_3 (%)**
Glacially polished ridge Elliði				
ELLID-1	7.20 ± 0.14	0.14 ± 0.02	6.96 ± 0.35	24.28 ± 0.49
ELLID-2	7.01 ± 0.14	0.12 ± 0.02	7.18 ± 0.36	25.12 ± 0.50
Moraine boulders of Hóladalur				
HOL-1	12.05 ± 0.24	0.29 ± 0.04	2.53 ± 0.13	13.16 ± 0.26
HOL-2	11.07 ± 0.22	0.35 ± 0.05	2.93 ± 0.15	14.13 ± 0.28
Fremri-Grjótárdalur rock glacier complex				
FGD-1	11.01 ± 0.22	0.28 ± 0.04	2.66 ± 0.13	14.07 ± 0.28
FGD-2	11.57 ± 0.23	0.33 ± 0.05	2.52 ± 0.13	12.79 ± 0.26
FGD-11	10.92 ± 0.22	0.28 ± 0.04	2.59 ± 0.13	13.70 ± 0.27
FGD-1B	11.37 ± 0.23	0.33 ± 0.05	3.15 ± 0.16	12.68 ± 0.25
FGD-2B	11.73 ± 0.23	0.31 ± 0.05	2.80 ± 0.14	10.60 ± 0.21
FGD-3B	9.88 ± 0.20	0.31 ± 0.05	4.06 ± 0.20	16.71 ± 0.33
FGD-4B	8.59 ± 0.17	0.40 ± 0.06	4.55 ± 0.23	19.70 ± 0.39
FGD-5B	8.96 ± 0.18	0.29 ± 0.04	4.75 ± 0.24	20.58 ± 0.41
Hofsjökull debris-covered glacier				
HOFS-1	9.91 ± 0.20	0.39 ± 0.06	3.54 ± 0.18	17.06 ± 0.34
HOFS-2	9.66 ± 0.19	0.39 ± 0.06	4.50 ± 0.22	18.43 ± 0.37
HOFS-3	9.63 ± 0.19	0.44 ± 0.07	4.37 ± 0.22	18.07 ± 0.36
Héðinsdalsjökull debris-covered glacier				
HEDIN-1	10.28 ± 0.21	0.18 ± 0.03	3.70 ± 0.18	16.91 ± 0.34
HEDIN-2	7.87 ± 0.16	0.80 ± 0.04	2.65 ± 0.13	13.36 ± 0.27
HEDIN-3	8.06 ± 0.16	0.76 ± 0.04	3.05 ± 0.15	14.50 ± 0.29

Table 4. Chemical composition of the bulk rock samples before chemical treatment.

Sample name	CaO (%)	K_2O (%)	TiO_2 (%)	Fe_2O_3 (%)	SiO_2 (%)	Na_2O (%)	MgO (%)	Al_2O_3 (%)	MnO (%)	P_2O_5 (%)	Li (ppm)	B (ppm)	Sm (ppm)	Gd (ppm)	Th (ppm)	U (ppm)	Cl (ppm)
Glacially polished ridge Elliði																	
ELLID-1	8.568	0.179	4.753	18.215	44.950	2.161	7.475	12.416	0.228	0.20	4.4	2	5.709	5.953	0.504	0.149	21
Fremri-Grjótárdalur rock glacier complex																	
FGD-1B	11.738	0.356	2.590	13.300	47.670	2.395	6.702	13.844	0.194	0.24	4.3	< 2	5.120	5.280	1.131	0.314	37
FGD-4B	9.580	0.465	3.529	16.270	47.200	2.808	5.223	12.798	0.239	0.34	6.1	< 2	6.930	7.122	1.605	0.437	44
Hofsjökull debris-covered glacier																	
HOFS-1	9.345	0.359	4.267	18.150	48.770	2.225	5.772	10.288	0.250	< L.D	5.4	< 2	2.756	3.213	1.017	0.336	77
Héðinsdalsjökull debris-covered glacier																	
HEDIN-1	10.773	0.262	2.880	14.920	47.290	2.282	6.423	12.918	0.213	0.24	4.4	< 2	5.447	5.704	1.143	0.317	40

Table 5. ^{36}Cl CRE dating results. The numbers in italics correspond to the internal (analytical) uncertainty at one standard level.

Sample name	**Sample weight (g)**	**Mass of Cl in spike (mg)**	**^{35}Cl/^{37}Cl**	**^{36}Cl/^{35}Cl (10^{-14})**	**[Cl] in sample (ppm)**	**[^{36}Cl] (10^4 atoms g^{-1})**	**^{36}Cl CRE age (yr)**
Glacially polished ridge Elliði							
ELLID-1	28.88	1.864	64.854 ± 0.615	11.051 ± 0.438	3.5	12.438 ± 0.516	16254 ± 1685 (*1217*)
ELLID-2	27.69	1.928	86.476 ± 0.876	10.014 ± 0.437	2.6	11.977 ± 0.547	16174 ± 1713 (*925*)
Moraine boulders of Hóladalur							
HOL-1	30.41	1.012	10.718 ± 0.037	17.257 ± 0. 435	15.6	15.060 ± 0.384	11096 ± 1092 (*1057*)
HOL-2	30.89	0.992	9.528 ± 0.066	15.669 ± 0.364	18.3	14.055 ± 0.336	10328 ± 993 (*668*)
Fremri-Grjótárdalur rock glacier complex							
FGD-1	31.96	1.018	7.805 ± 0.131	13.071 ± 0.399	25.7	13.311 ± 0.444	10534 ± 1048 (*720*)
FGD-2	30.2	0.985	6.026 ± 0.035	13.066 ± 0.395	43.9	17.536 ± 0.547	11092 ± 1111 (*734*)
FGD-11	30.69	1.000	9.585 ± 0.096	17.206 ± 0.568	18.4	15.604 ± 0.525	11341 ± 1133 (*782*)
FGD-1B	70.54	1.883	6.135 ± 0.648	48.960 ± 0.269	36.7	4.304 ± 0.287	2509 ± 290 (*227*)
FGD-2B	70.34	1.880	5.649 ± 0.646	83.750 ± 0.343	43.8	8.330 ± 0.444	5176 ± 565 (*411*)
FGD-3B	67.66	1.882	5.888 ± 0.568	10.512 ± 0.412	41.6	10.414 ± 0.521	6546 ± 696 (*505*)
FGD-4B	26.52	1.851	14.293 ± 0.150	87.158 ± 0.394	25.1	12.908 ± 0.627	9274 ± 951 (*715*)
FGD-5B	25.78	1.870	11.531 ± 0.115	86.801 ± 0.361	35	14.353 ± 0.655	9450 ± 977 (*706*)
Hofsjökull debris-covered glacier							
HOFS-1	84.09	1.822	4.289 ± 0.532	68.219 ± 0.356	77.4	9.128 ± 0.670	5417 ± 669 (*509*)
HOFS-2	85.46	1.832	5.189 ± 0.100	89.175 ± 0.466	43.0	8.026 ± 0.552	5596 ± 644 (*508*)
HOFS-3	86.23	1.819	4.374 ± 0.671	90.595 ± 0.430	70.2	11.279 ± 0.809	6748 ± 817 (*625*)
Héðinsdalsjökull debris-covered glacier							
HEDIN-1	67.56	1.878	8.846 ± 0.853	45.314 ± 0.258	19.9	3.167 ± 0.202	2953 ± 334 (260)
HEDIN-2	64.38	1.875	4.706 ± 0.454	25.226 ± 0.165	76.5	3.571 ± 0.286	2591 ± 337 (266)
HEDIN-3	63.98	1.893	4.717 ± 0.438	22.065 ± 0.157	77.1	3.136 ± 0.269	2221 ± 300 (241)
Blanks [a]					*Total atoms Cl* (10^{17})	*Total atoms ^{36}Cl* (10^4)	
BK-1		1.800	297.029 ± 11.372	0.545 ± 0.097	2.941 ± 0.220	16.981 ± 3.034	
BK-2		1.884	356.675 ± 7.637	0.575 ± 0.135	2.313 ± 0.139	18.738 ± 4.384	
BK-3		1.888	328.059 ± 2.892	0.359 ± 0.069	2.650 ± 0.136	11.725 ± 2.249	
Cblk3125-1		1.897	98.243 ± 1.536	14.248 ± 0.301			
Cblk3125-2		1.859	85.103 ± 0.398	2.228 ± 0.175			

[a] BK-1 was processed with samples HOFS-1, HOFS-2 and HOFS-3; BK-2 was processed with samples FGD-1B, FGD-2B and FGD-3B; BK-3 was processed with samples ELLID-1, ELLID-2, HEDIN-1, HEDIN-2, HEDIN-3, FGD-4B and FGD-5B. Cblk3125-1 and Cblk3125-2 were processed with the other samples.

1387

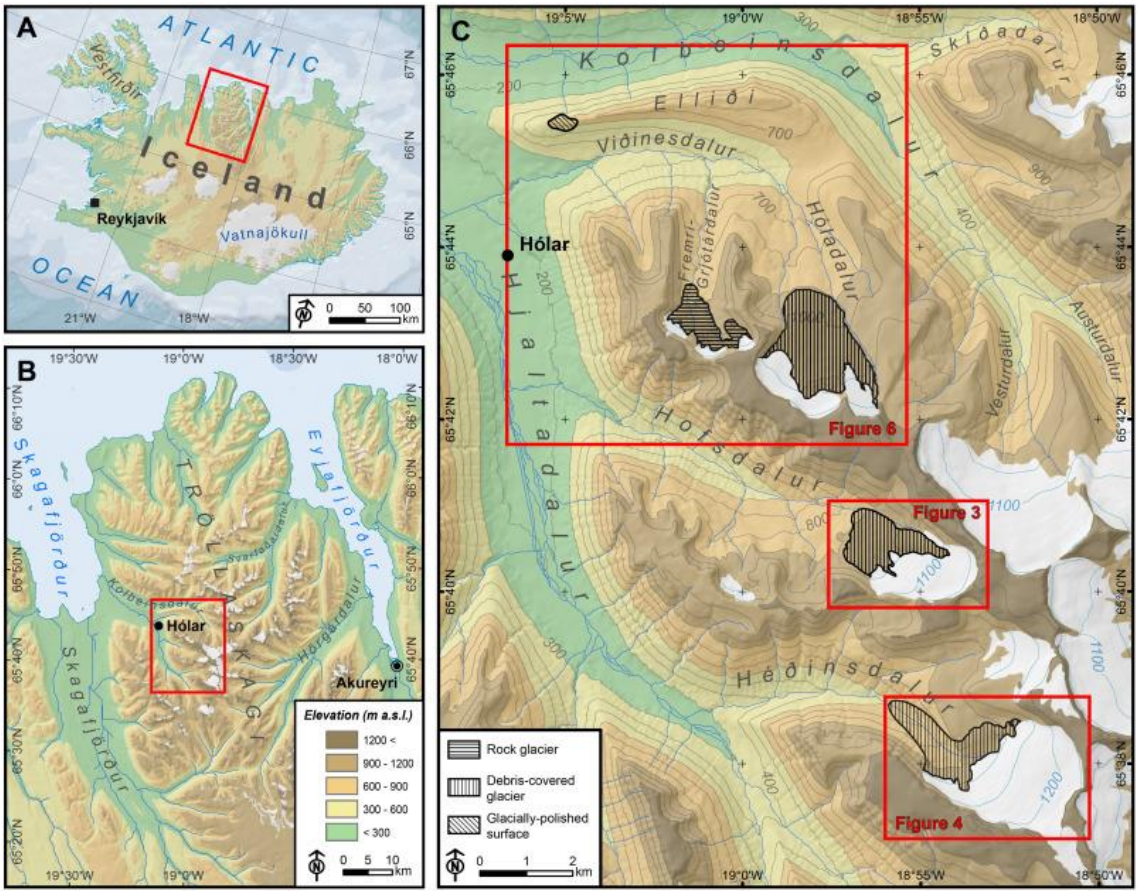

1388

1389

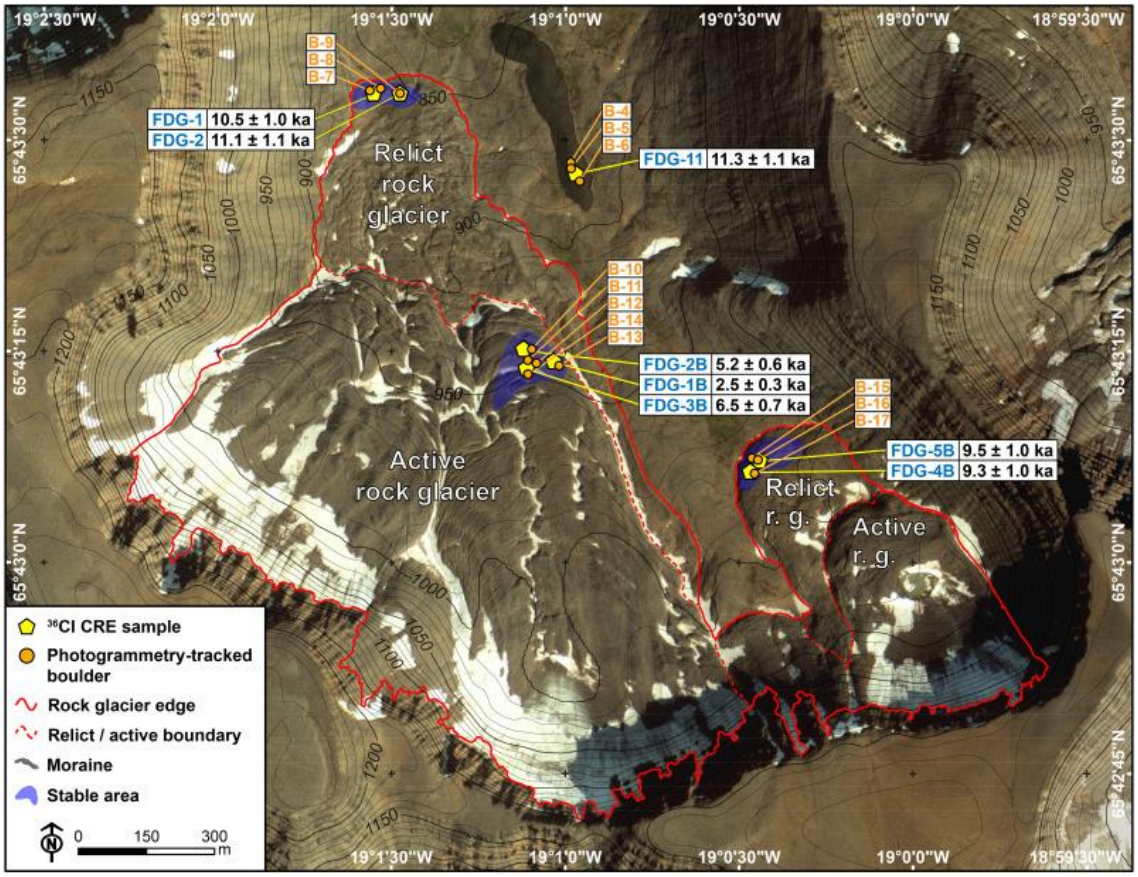
19°2'30"W
19°2'0"W
19°1'30"W
19°1'0"W
19°0'30"W
19°0'0"W
18°59'30"W
65°43'30"N
65°43'15"N
65°43'0"N
65°42'45"N
B-9
B-8
B-7
FDG-1 10.5 ± 1.0 ka
FDG-2 11.1 ± 1.1 ka
Relict rock glacier
B-4
B-5
B-6
FDG-11 11.3 ± 1.1 ka
B-10
B-11
B-12
B-14
B-13
FDG-2B 5.2 ± 0.6 ka
FDG-1B 2.5 ± 0.3 ka
FDG-3B 6.5 ± 0.7 ka
Active rock glacier
B-15
B-16
B-17
FDG-5B 9.5 ± 1.0 ka
FDG-4B 9.3 ± 1.0 ka
Relict r. g.
Active r. g.
36Cl CRE sample
Photogrammetry-tracked boulder
Rock glacier edge
Relict / active boundary
Moraine
Stable area
0
150
300
m

1390

1391

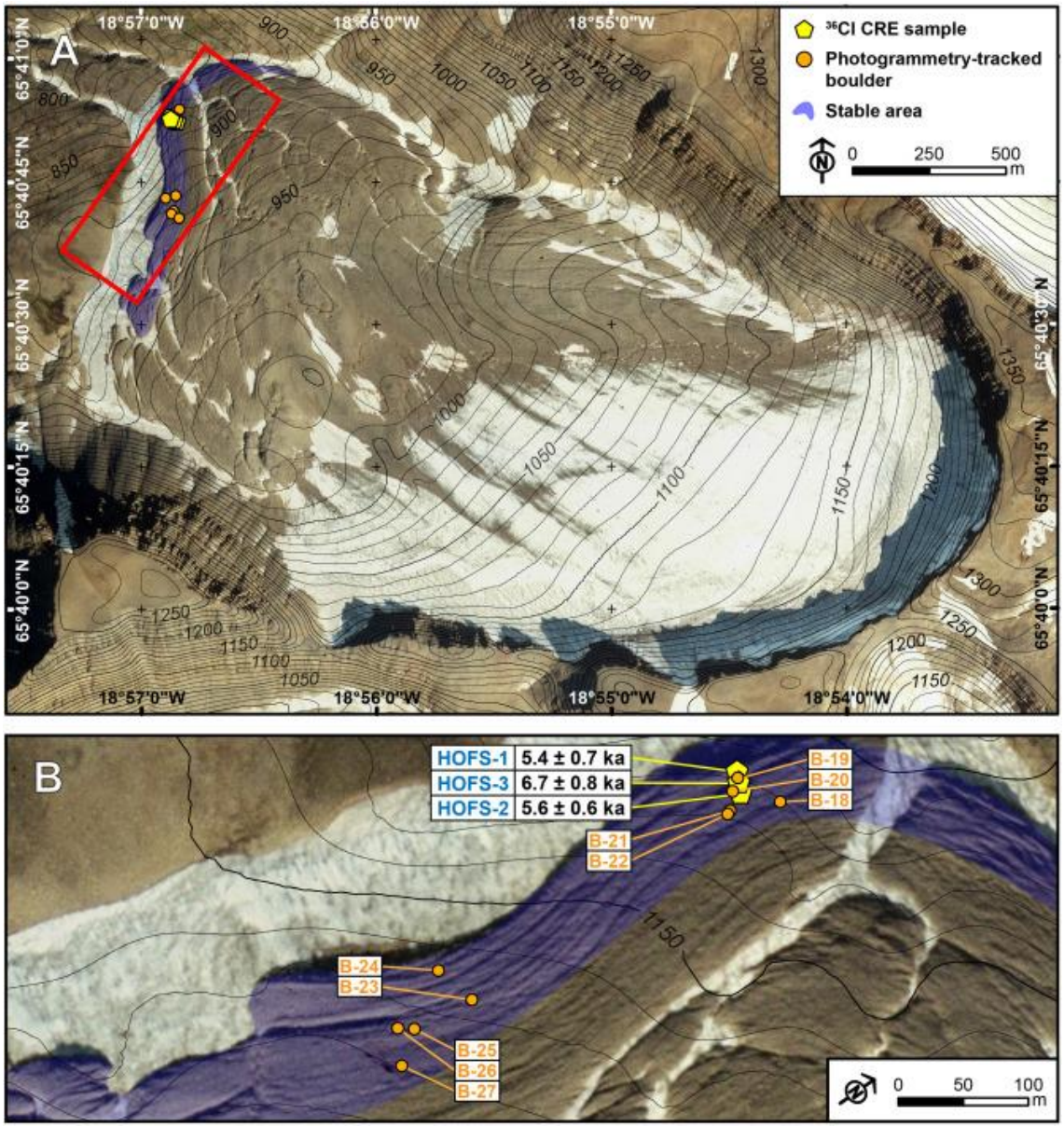
A
18°57'0"W
18°56'0"W
18°55'0"W
18°54'0"W
65°41'0"N
65°40'45"N
65°40'30"N
65°40'15"N
65°40'0"N
36Cl CRE sample
Photogrammetry-tracked boulder
Stable area
0 250 500 m
B
HOFS-1 5.4 ± 0.7 ka
HOFS-3 6.7 ± 0.8 ka
HOFS-2 5.6 ± 0.6 ka
B-19
B-20
B-18
B-21
B-22
B-24
B-23
B-25
B-26
B-27
0 50 100 m

1392

1393

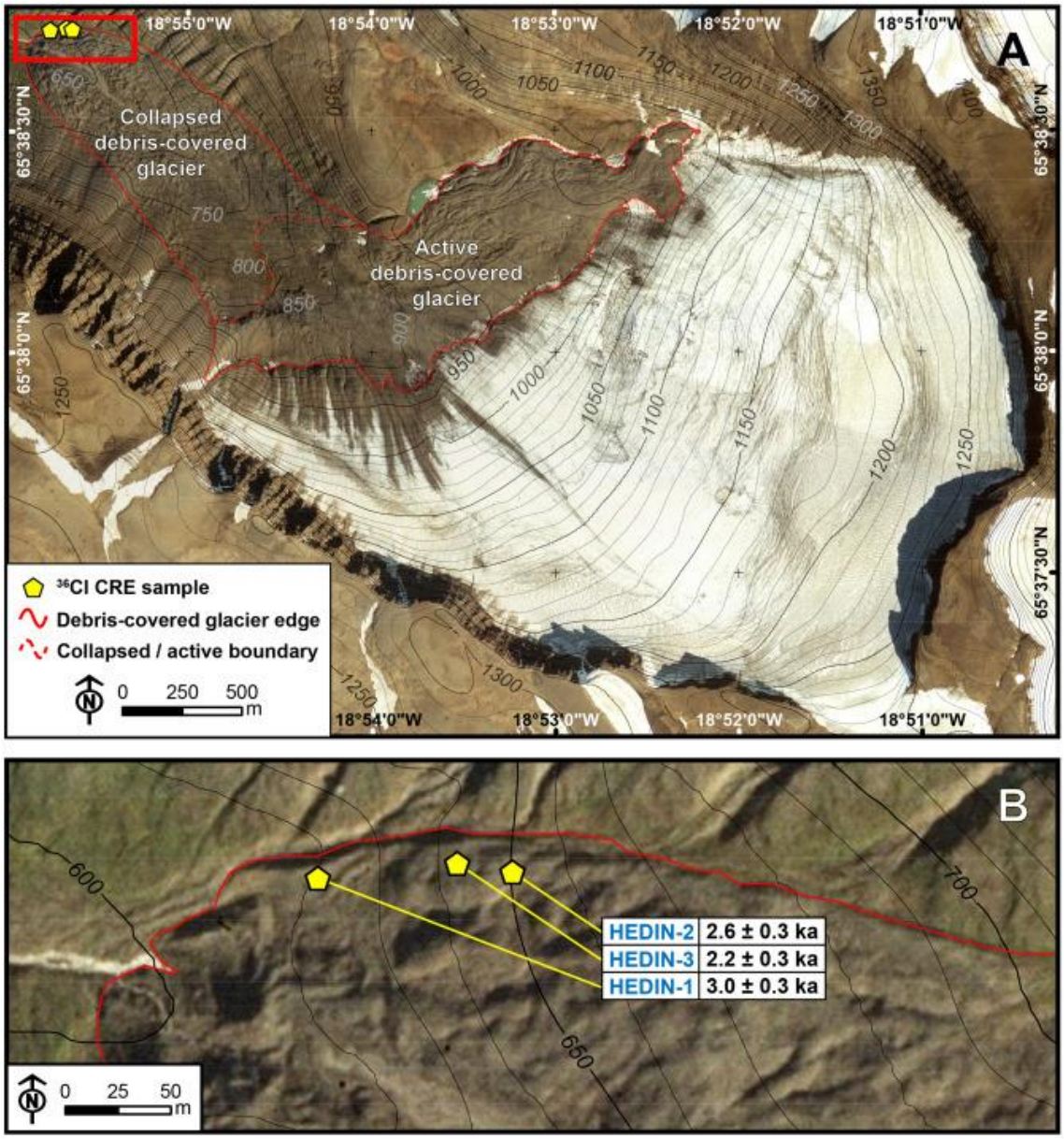
A
Collapsed debris-covered glacier
Active debris-covered glacier
36Cl CRE sample
Debris-covered glacier edge
Collapsed / active boundary
0 250 500 m
18°55'0"W
18°54'0"W
18°53'0"W
18°52'0"W
18°51'0"W
65°38'30"N
65°38'0"N
65°37'30"N
B
HEDIN-2 2.6 ± 0.3 ka
HEDIN-3 2.2 ± 0.3 ka
HEDIN-1 3.0 ± 0.3 ka
0 25 50 m

1394

1395

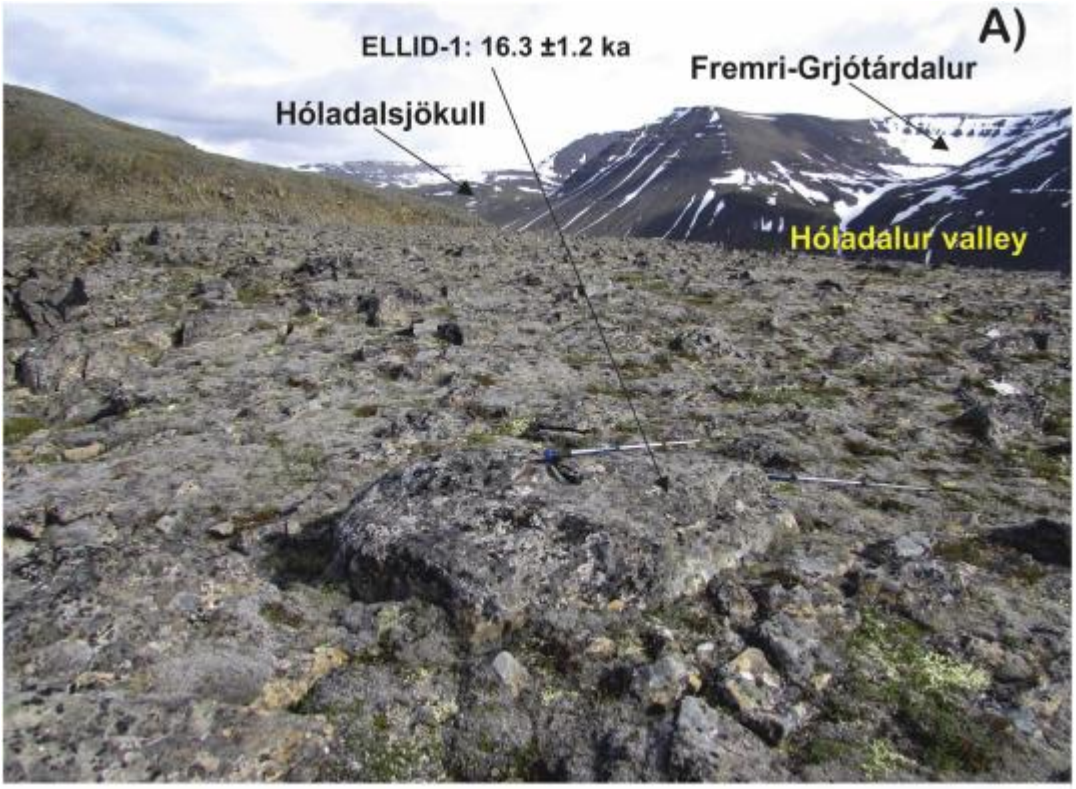
A)
ELLID-1: 16.3 ±1.2 ka
Fremri-Grjótárdalur
Hóladalsjökull
Hóladalur valley

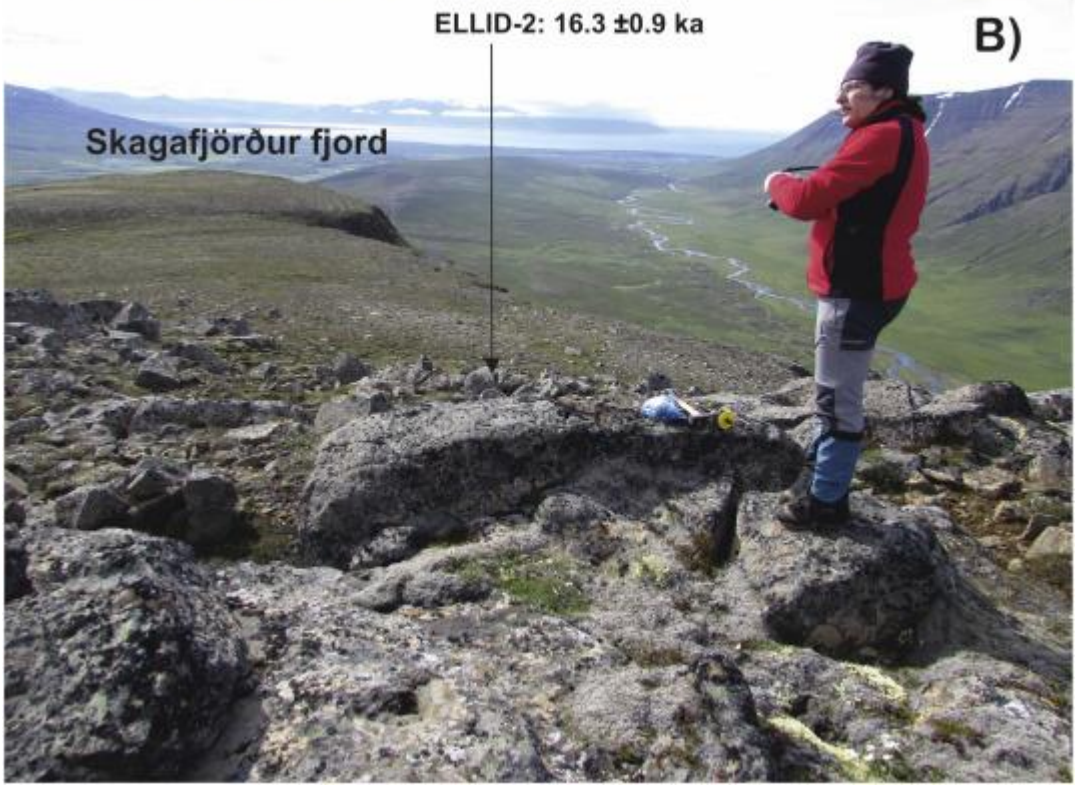
B)
ELLID-2: 16.3 ±0.9 ka
Skagafjörður fjord

1396

1397

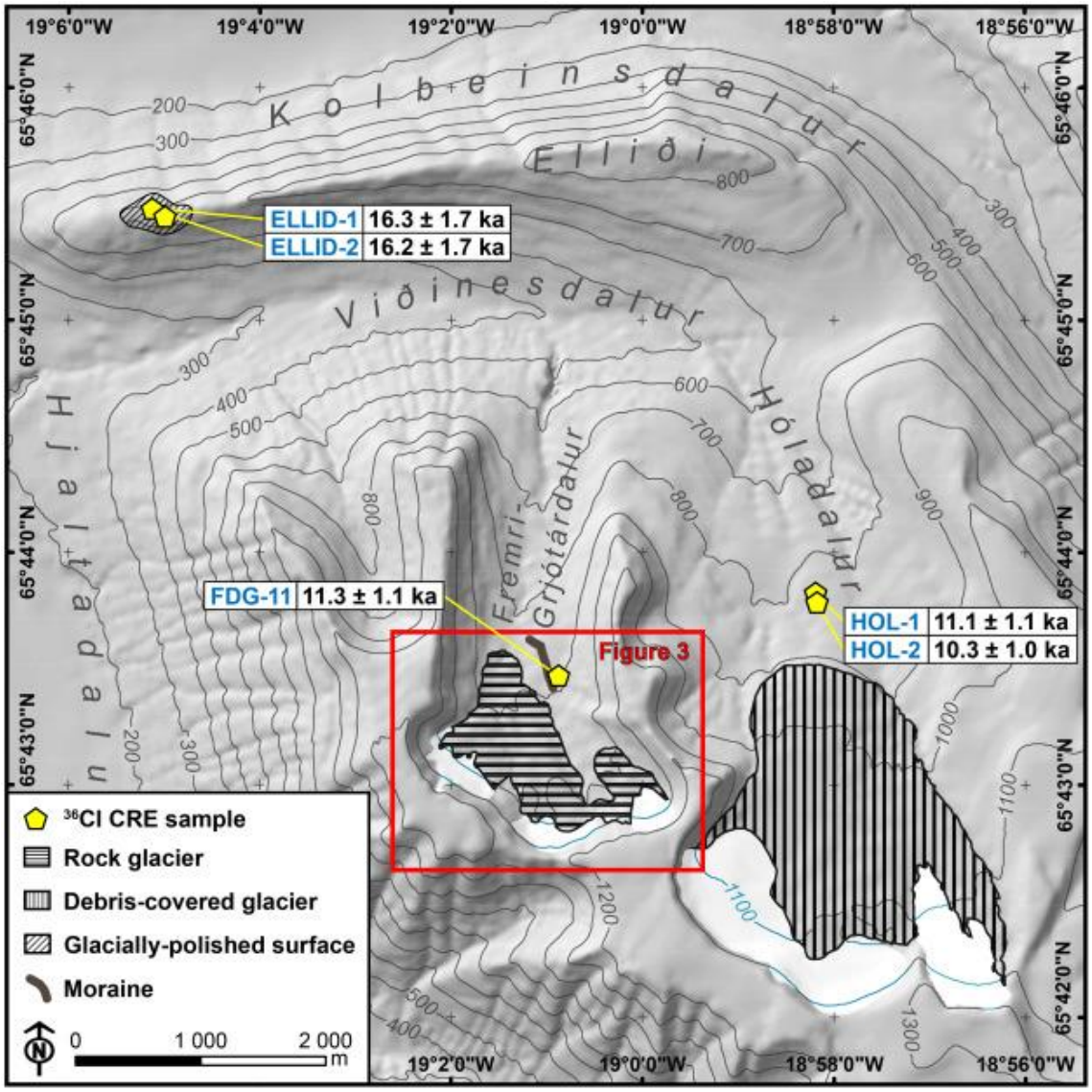
19°6'0"W
19°4'0"W
19°2'0"W
19°0'0"W
18°58'0"W
18°56'0"W
65°46'0"N
65°45'0"N
65°44'0"N
65°43'0"N
65°42'0"N
Kolbeinsdalur
Elliði
Viðinesdalur
Hjaltadalur
Hóladalur
Fremri-Grjótárdalur
ELLID-1 16.3 ± 1.7 ka
ELLID-2 16.2 ± 1.7 ka
FDG-11 11.3 ± 1.1 ka
HOL-1 11.1 ± 1.1 ka
HOL-2 10.3 ± 1.0 ka
Figure 3
36Cl CRE sample
Rock glacier
Debris-covered glacier
Glacially-polished surface
Moraine
0
1 000
2 000
m

1398

1399

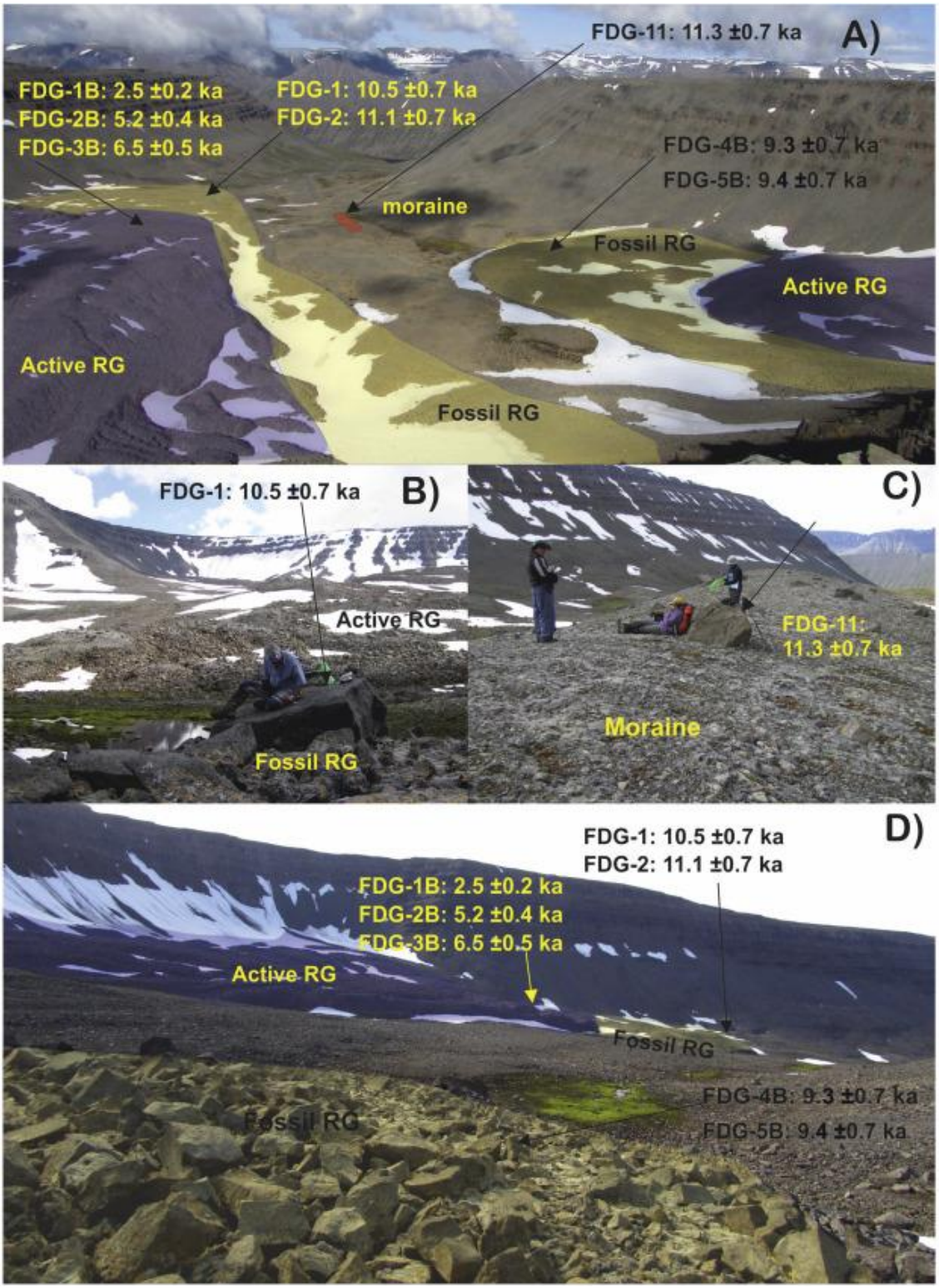
A)
FDG-11: 11.3 ±0.7 ka
FDG-1B: 2.5 ±0.2 ka
FDG-2B: 5.2 ±0.4 ka
FDG-3B: 6.5 ±0.5 ka
FDG-1: 10.5 ±0.7 ka
FDG-2: 11.1 ±0.7 ka
FDG-4B: 9.3 ±0.7 ka
FDG-5B: 9.4 ±0.7 ka
moraine
Fossil RG
Active RG
Active RG
Fossil RG
B)
FDG-1: 10.5 ±0.7 ka
Active RG
Fossil RG
C)
FDG-11:
11.3 ±0.7 ka
Moraine
D)
FDG-1: 10.5 ±0.7 ka
FDG-2: 11.1 ±0.7 ka
FDG-1B: 2.5 ±0.2 ka
FDG-2B: 5.2 ±0.4 ka
FDG-3B: 6.5 ±0.5 ka
Active RG
Fossil RG
FDG-4B: 9.3 ±0.7 ka
FDG-5B: 9.4 ±0.7 ka
Fossil RG

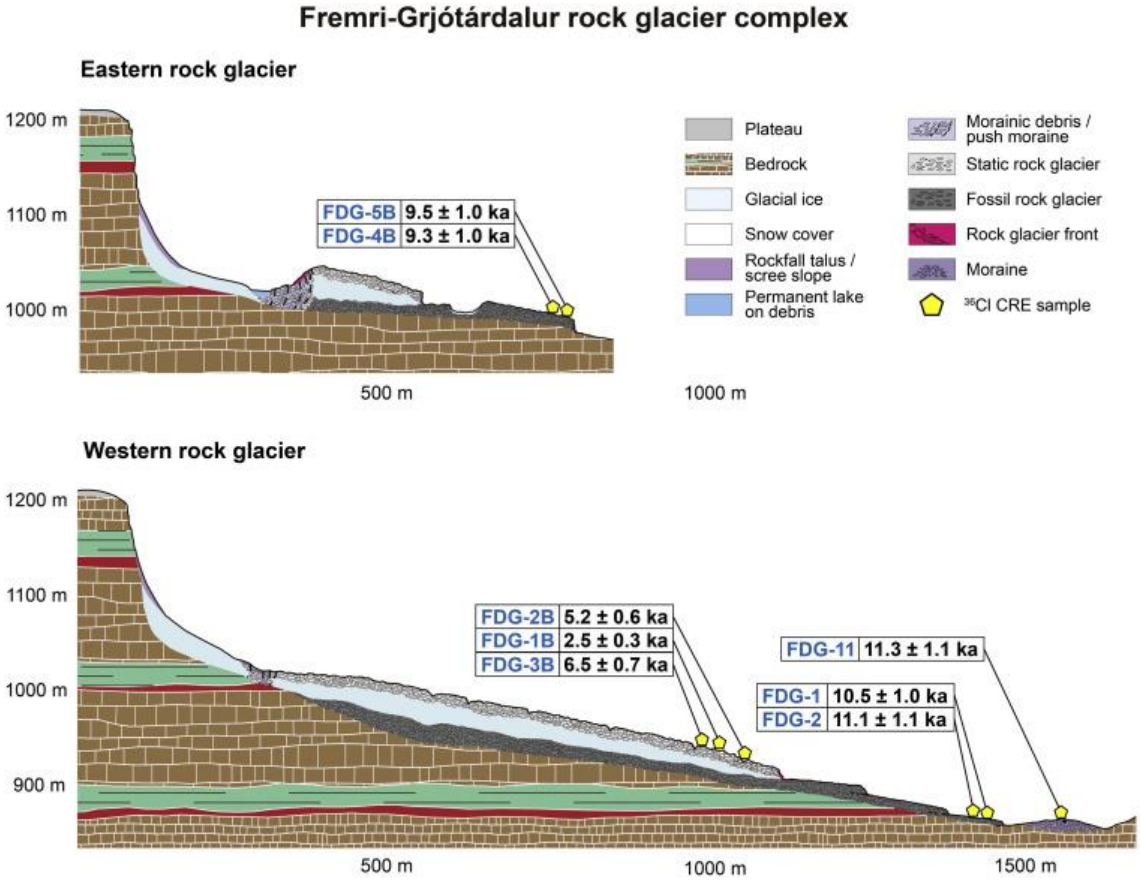
Fremri-Grjótárdalur rock glacier complex
Eastern rock glacier
1200 m
1100 m
1000 m
FDG-5B 9.5 ± 1.0 ka
FDG-4B 9.3 ± 1.0 ka
500 m
1000 m
Plateau
Bedrock
Glacial ice
Snow cover
Rockfall talus / scree slope
Permanent lake on debris
Morainic debris / push moraine
Static rock glacier
Fossil rock glacier
Rock glacier front
Moraine
36Cl CRE sample
Western rock glacier
1200 m
1100 m
1000 m
900 m
FDG-2B 5.2 ± 0.6 ka
FDG-1B 2.5 ± 0.3 ka
FDG-3B 6.5 ± 0.7 ka
FDG-11 11.3 ± 1.1 ka
FDG-1 10.5 ± 1.0 ka
FDG-2 11.1 ± 1.1 ka
500 m
1000 m
1500 m

1402

1403

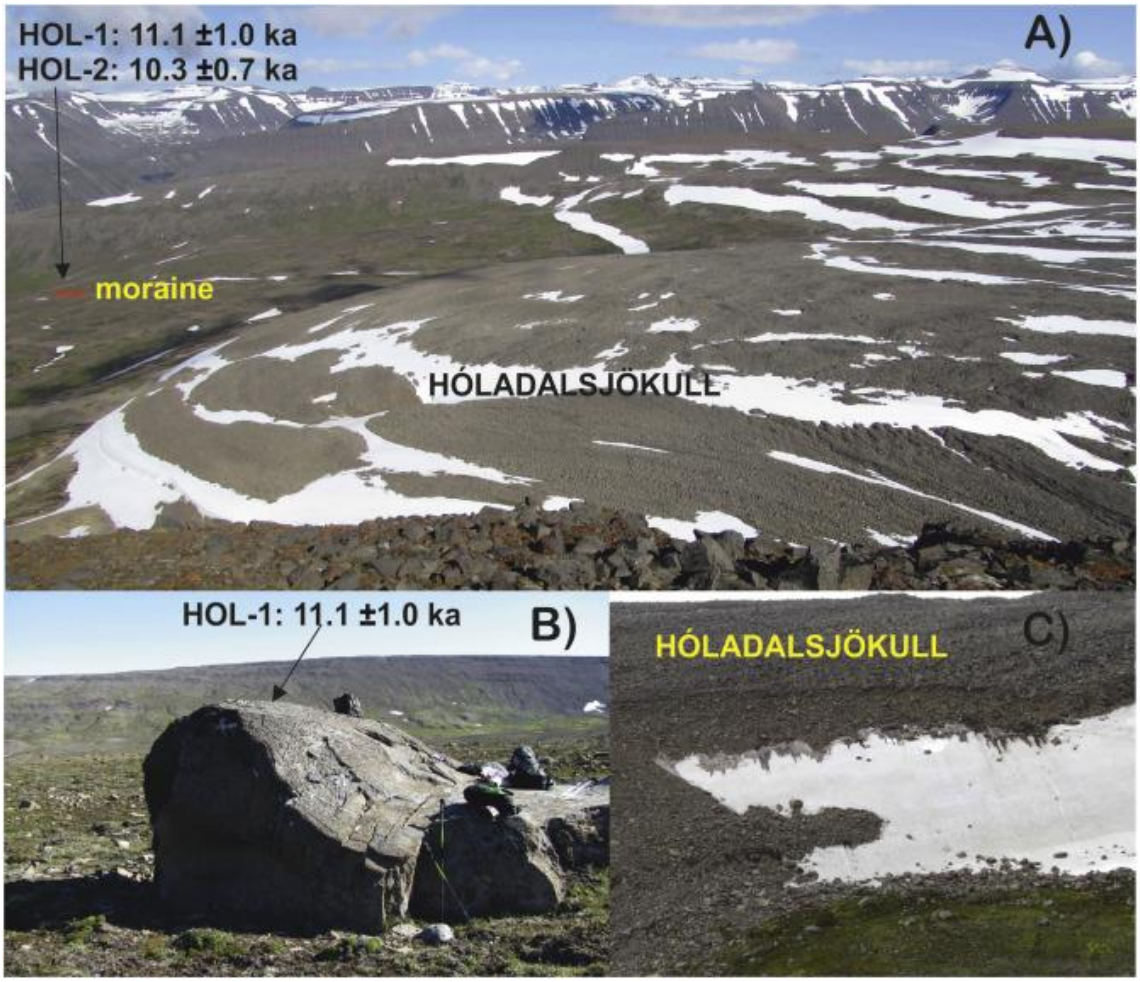
HOL-1: 11.1 ±1.0 ka
HOL-2: 10.3 ±0.7 ka
A)
moraine
HÓLADALSJÖKULL
HOL-1: 11.1 ±1.0 ka
B)
HÓLADALSJÖKULL
C)

1404

1405

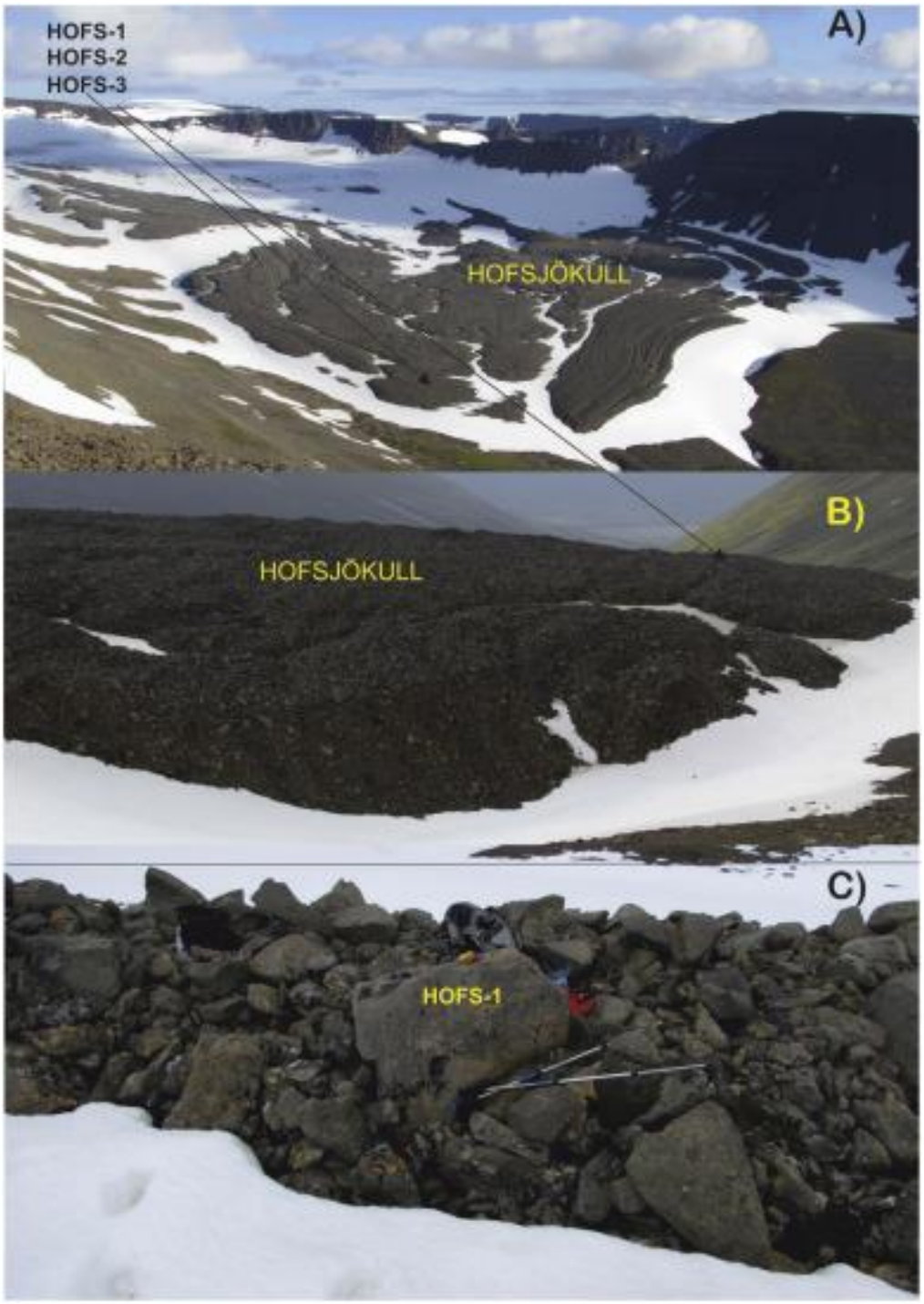

1406

1407

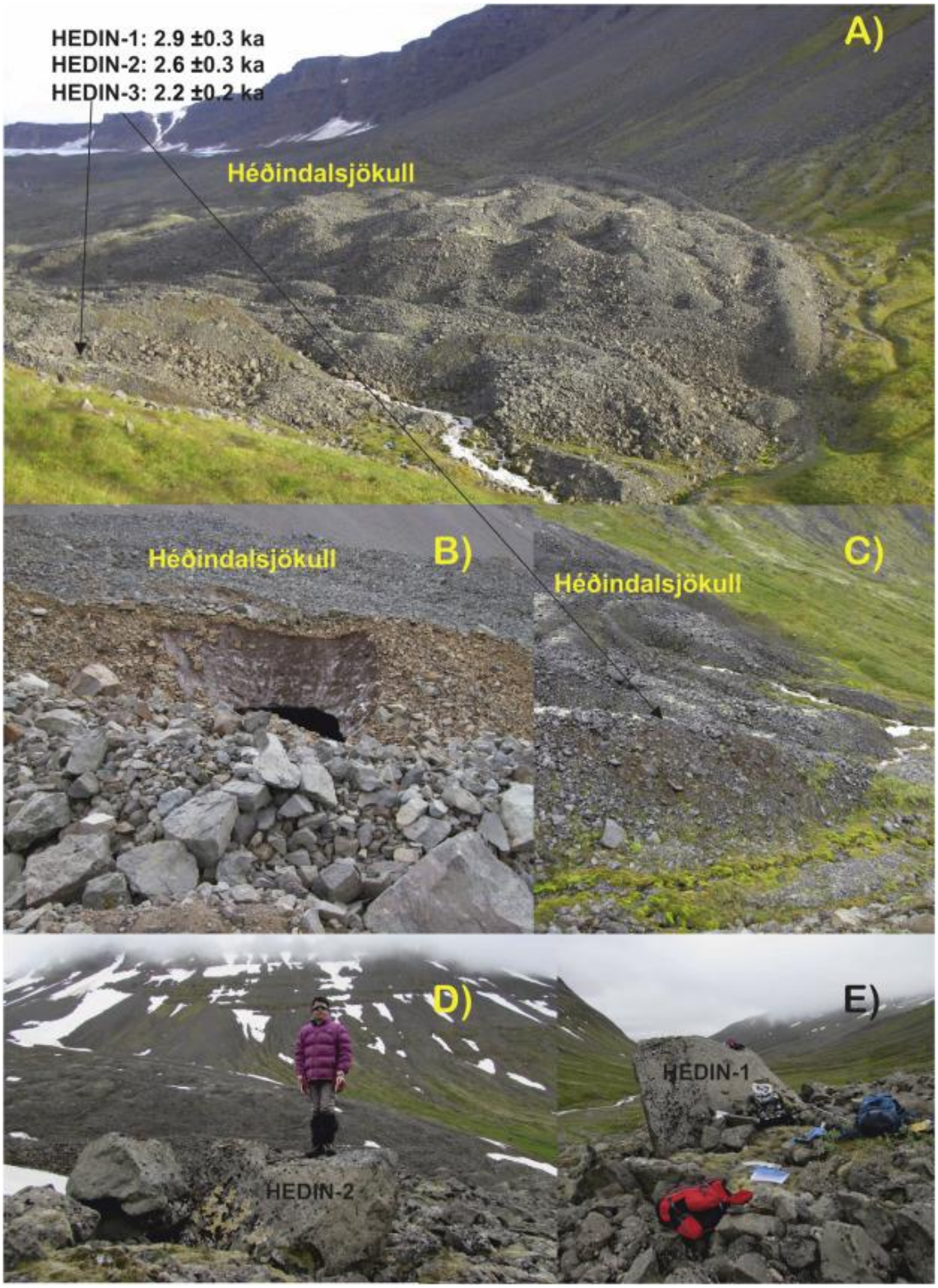
HEDIN-1: 2.9 ±0.3 ka
HEDIN-2: 2.6 ±0.3 ka
HEDIN-3: 2.2 ±0.2 ka
A)
Héðindalsjökull
Héðindalsjökull
B)
Héðindalsjökull
C)
D)
HEDIN-2
E)
HEDIN-1

1408

1409

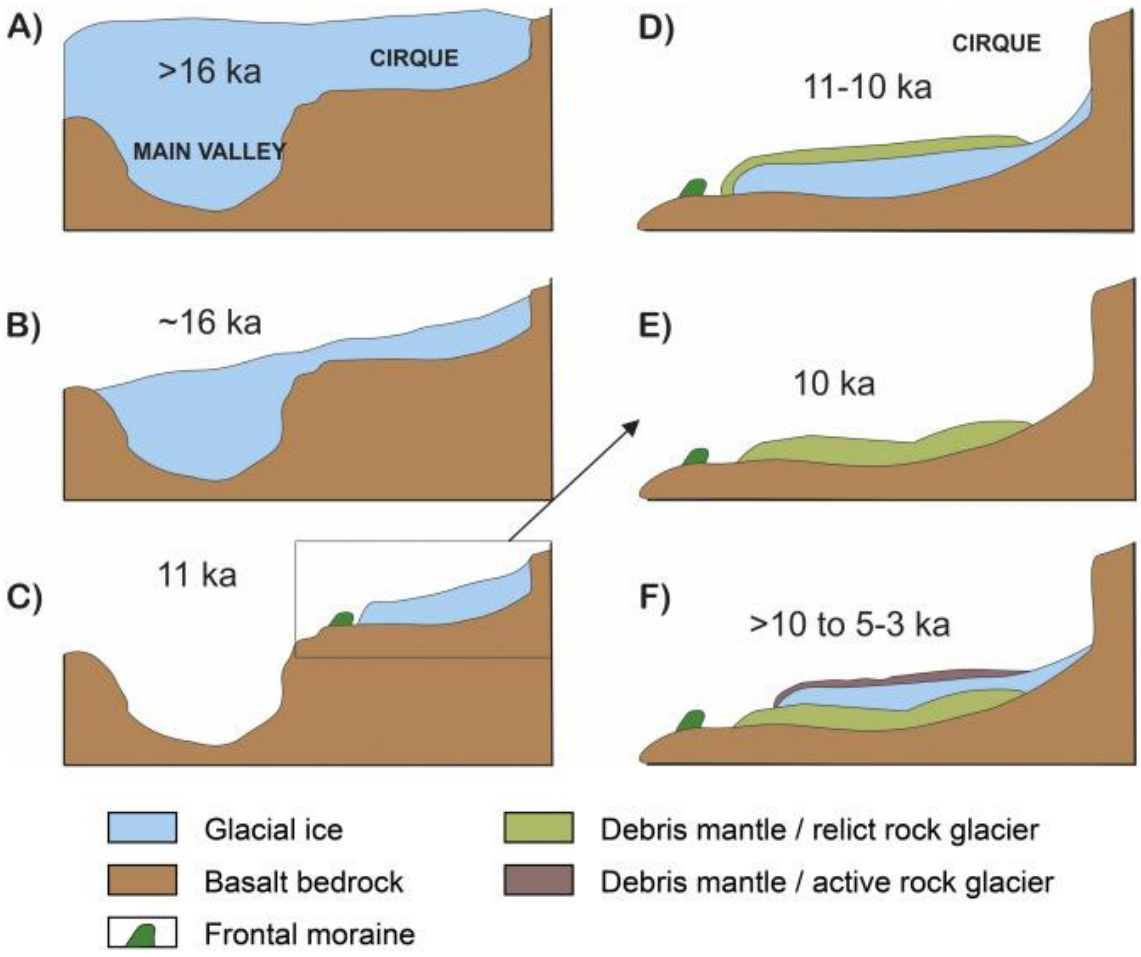
A)
>16 ka
CIRQUE
MAIN VALLEY
B)
~16 ka
C)
11 ka
D)
CIRQUE
11-10 ka
E)
10 ka
F)
>10 to 5-3 ka
Glacial ice
Basalt bedrock
Frontal moraine
Debris mantle / relict rock glacier
Debris mantle / active rock glacier

1410

1411

Figure captions

Figure 1. Location of the study area in central north Iceland (A) the Tröllaskagi peninsula (B) and glaciers and debris-covered glaciers under study (C). The red boxes show the extent of the aerial photos and maps corresponding to the Fig. 2, Fig. 3, Fig. 6.

Figure 2. View of the Fremri-Grjótárdalur rock glacier complex and spatial distribution of ^{36}Cl CRE samples and photogrammetry-tracked boulders. Stable area refers where it is known that the boulder movement of <0.16 m yr^{-1}. The red dashed line indicates the edge between the relict and active rock glaciers.

Figure 3. Overhead view of the Hofsjökull glacier complex and spatial distribution of ^{36}Cl CRE samples and photogrammetry-tracked boulders. Panel A shows the whole glacier complex (debris-free and debris-covered sectors). Panel B is a zoom of the frontal area. Stable area refers where it is known that the boulder movement is <0.37 m yr^{-1}.

Figure 4. View of the Héðinsdalsjökull glacier complex and spatial distribution of ^{36}Cl CRE samples and photogrammetry-tracked boulders. Panel A shows the whole glacier complex (debris-free and fossil/active debris-covered sectors). Panel B is a zoom of the frontal area. The red dashed line in panel A indicates the edge between the collapsed and active debris-covered glaciers.

Figure 5. A) Location of sample ELLID-1 viewed from the west, on the northern side of the Hóladalur valley. Hólajökull and Fremri-Grjótárdalur cirques at the bottom. B) Location of sample ELLID-2 viewed from the east. The Skagafjörður fjord can be seen at the bottom. Ages results from samples: ELLID-1: 16.3 ± 1.2 ka; ELLID-2: 16.3 ± 0.9 ka.

Figure 6. Location of samples describing the deglaciation pattern of the study area. The red box corresponds to the extent of the Fig. 2.

1436 Figure 7. Photos of the Fremri-Grjótárdalur rock glacier complex. A) View of the rock
1437 glacier complex from the summit area to the north. B) Sample FDG-1 in the relict rock
1438 glacier. C) Sample FDG-11 in the lateral moraine located in front of the rock glaciers. D)
1439 View of the rock glacier complex from the eastern sector of the cirque.

1440 Figure 8. Idealized longitudinal profile of the Fremri-Grjótárdalur rock glaciers and the
1441 relative position of the ^{36}Cl CRE samples. The inner structure is speculative.

1442 Figure 9. ield photos of Hóladalur cirque. A) Oblique view of the Hóladalsjökull debris-
1443 covered glacier from the western summit area. B) Sample HOL-1 in a moraine in front of
1444 the debris-covered glacier. C) Close up view of the debris-covered glacier snout.

1445 Figure 10. Field photos of Hofsjökull cirque. A) Oblique view of the Hofsjökull debris-
1446 covered glacier from the southern summit area. B) Close up view of the debris-covered
1447 glacier snout. C) Sample HOFS-1 on a crest located in the frontal area of the debris-
1448 covered glacier.

1449 Figure 11. Field photos of Héðinsdalsjökull glacier. A) Oblique view of the
1450 Héðinsdalsjökull debris-covered glacier from the south. B) Middle sector of the debris-
1451 covered glacier with internal ice. C) Snout of the debris-covered glacier in the current
1452 fossil stage. D) Sample HEDIN-2 on a crest in the frontal area of the debris-covered
1453 glacier. E) Sample HEDIN-1 on the crest in the frontal area of the debris-covered glacier.

1454 Figure 12. dealized model about the evolution of glaciers in the Tröllaskagi mountains
1455 according to the CRE dating results. A) The main valleys of the interior of Tröllaskagi
1456 were covered with ice before 16 ka, feeding the glacier outlet of Skagafjörður. B) Around
1457 16 ka a series begins of rapid, intense, glaciological and geomorphological processes; the
1458 sequence can be determined, but the uncertainty of the CRE results prevents an accurate
1459 timing of each specific moment. Deglaciation begins around 16 ka and glaciers in the

interior of Tröllaskagi become disconnected from the Skagafjörður glacier outlet. C) Subsequently, the main valleys are deglaciated with a small advance inside the cirques around 11 ka. D) The first rock glacier generation forms around 11–10 ka. E) The glacier fronts rapidly become inactive around 10 ka. F) After 10 ka, a new generation of rock glaciers forms and their dynamics begin to stabilize 5–3 ka according to their altitude. Note that the debris mantle of the stage D contributed to form the deposits of the relict rock glacier of the following stage E.